JOURNAL OF COMPUTATIONAL PHYSICS 43, 111–163 (1981)

Algorithms for the Self-Consistent Generation of Magnetic Fields in Plasmas

G. J. PERT

Department of Applied Physics, The University of Hull, Hull Hu6 7RX, England

Received April 25, 1979; revised December 1, 1980

The generation, advection and diffusion of magnetic fields in cylindrically symmetric plasmas is considered. Stable and conservative numerical schemes for treating this problem within the framework of a conventional multi-celled fluid code are presented.

1. INTRODUCTION

The observation of strong magnetic fields associated with the plasmas generated by strong laser irradiation of solid targets has led to considerable interest in the self-generation of magnetic fields within the plasma. Initial theory considered only the effects of the electron pressure as source [1, 2]. More recently it has been shown that the thermo-electric terms [3, 4] can contribute significantly. In addition, further sources directly associated with the laser [5, 6] may also be present in a given experiment. In this paper we shall consider only the internal electron pressure and thermo-electric sources of the field. The inclusion of further external sources is trivial and easily incorporated with the schemes described in this paper.

Since the magnetic field is intimately related to gradients in the electron density and temperature, it is clear that the fields only develop in an evolving plasma. Thus in any realistic situation one must solve the magnetic field equations consistently with those of the plasma hydrodynamics. Furthermore, since the fields are only produced in a plasma with non-parallel electron density and temperature gradients, it is clear that the hydrodynamics must be solved in at least a two dimensional flow. This involves a typical two dimensional cell-type calculation, which may be in Eulerian or Lagrangian geometry. This problem is best treated in Eulerian geometry, and a number of satisfactory hydrodynamic schemes are available [7–10].

In this paper we shall assume that the incoming laser radiation is cylindrically symmetric. This allows the problem to be treated in cylindrical (two dimensional) geometry, with a considerable saving in computer effort. Under these circumstances the only magnetic field component is azimuthal [3], the lines of force forming circular loops about the axis. By symmetry the flux density must be zero on the axis ($B = 0$, at $r = 0$).

0021-9991/81/090111-53$02.00/0

581/43/1-8

This problem has been treated in a number of different ways by various authors [11–14]. In this paper we shall present a scheme which allows the computations to maintain the conservation properties of the physical quantities involved, and yet entails a minimum of storage, only the flow variables being used in the calculation. Furthermore efforts are made to allow the use of as large a time-step as possible, within the constraints of the hydrodynamics, to reduce the total running time of the code.

Such a programme clearly has many similarities with those developed for magneto-hydrodynamic flows [15, 16]. Lindemuth [17] has drawn attention to the difficulty of maintaining energy conservation in these schemes, and has shown how this may be done. The finite difference schemes used here closely resemble those proposed by Lindemuth [17] in the use of face-centred differences, and have the same conservation properties.

In this paper we shall first examine the basic form of the differential equations governing these phenomena. Being essentially the equations of magneto-hydrodynamics, these relations express general conservation laws of mass, momentum, energy and magnetic flux. In view of this it is natural to identify terms which are coupled through these conservation laws, such as, for example, the magnetic diffusion/Ohmic heating terms in the magnetic field and electron energy equations: the finite difference relations are later developed in these complementary terms. The governing equations are also recast into a general conservative form in order to demonstrate the conservation relations.

In principle one would like to perform the calculation of the hydrodynamics, diffusion and magnetic field generation simultaneously within a single loop. The recent advances made in solving large sparse matrices by the ICCG method [18] make such a programme feasible, although it will make large demands on computer storage. Alternatively one can use an alternating direction integration (ADI) method to perform the calculation, as has been done for the standard magneto-hydrodynamic problem by Lindemuth and Killeen [16]. Such an approach, whilst it can be made to obey the governing conservation relations exactly, is made more difficult by the need to simultaneously solve three energy relaxation processes, magnetic, electron and ion thermal energies, and does not readily allow the use of a stiff form with a large effective time-step. To reduce the complexity of the problem it is advantageous to use the split time-step philosophy, and separate the various calculations into their complementary parts, which mutually maintain energy conservation.

It is clear from the above remarks that conservation relations must play an important role in assembling the finite difference relations to describe these phenomena. Unfortunately these are not the only essential physical constraints on the problem; a further important condition is that of positivity, particularly with regard to the individual energy terms. It is not possible to maintain strict positivity of *all* individual energy terms simultaneously with exact energy conservation, but only with a weaker conservation condition. One is therefore faced with a compromise either to maintain exact (strong) energy conservation, and eliminate positivity violations by an ad hoc procedure such as reset to zero, or to maintain positivity but allow some

conservation error. We have adopted the latter approach using algorithms for which the conservation error may be restricted to within a prescribed limit by an appropriate time-step control (weak conservation). Both exact (strong) and weak conservation forms of the algorithms will be given. These general conditions on conservation wll be discussed, and a simple stability theorem for such schemes derived.

Some effort has been made to set up the finite difference relations using a general approach in terms of face-centred differencing of the governing differential equations. The basic difference schemes used are described before proceeding to the treatment of specific terms in the equations, which are investigated within the time-splitting approximation.

The set of differential equations are split into interacting terms, which are differenced in such a way as to maintain the overall conservation laws of the exact solution. The splitting is accomplished into the following sets of equations: magnetic source, magnetic diffusion/Ohmic heating, thermal conduction, magnetic pressure and acceleration/magnetic flux convection. It is shown for stability most of these terms must be differenced implicitly. The resultant matrix equations are solved either by ICCG [18] (magnetic diffusion and thermal conduction) or by an ADI approach involving Newton–Raphson iteration (magnetic source). The inclusion of these terms in the working code MAGT is briefly described and some results illustrating its behaviour presented.

2

(i) *The Governing Equations*

The equations describing the self-generation of magnetic fields in plasmas were derived in Ref. [3]. However, for our purposes it is convenient to use slightly modified forms of the equations given previously, from which they are obtained by the use of vector identities. The equations will be given in Gaussian units with e the unsigned electron charge, c velocity of light and k Boltzmann's constant.

The growth of the magnetic flux density $\mathbf{B}$ in a plasma moving with velocity $\mathbf{v}$ and magnetic diffusivity tensor $\boldsymbol{\eta}$ (including the complete Hall term [3]) is given by

$$\frac{\partial \mathbf{B}}{\partial t} - \underbrace{\nabla \wedge (\mathbf{v} \wedge \mathbf{B})}_{\text{advection}} + \underbrace{\nabla \wedge [\boldsymbol{\eta} \cdot (\nabla \wedge \mathbf{B})]}_{\text{diffusion}} = \underbrace{\nabla \wedge \mathbf{S}}_{\text{source}} \tag{1}$$

where the terms are identified by the words below.

The source function may be written as:

$$\mathbf{S} = \frac{c}{e} \boldsymbol{\beta} \cdot \nabla(kT_e) \tag{2}$$

where the tensor $\boldsymbol{\beta}$, defined in Ref. [3], includes both the usual $\nabla n_e \wedge \nabla kT_e$ terms

and the thermo-electric diffusion tensor $\boldsymbol{\beta}$, whose values are given in Ref. [19] through

$$\beta_{||} = \beta_{||}^{\circ} - \ln(n_e), \qquad \beta_{\perp} = \beta_{\perp}^{\circ} - \ln(n_e), \qquad \beta_{\wedge} = \beta_{\wedge}^{\circ} \tag{3}$$

in the usual notation [19].

With this definition of the source function **S**, the most appropriate form of the electron energy equation is

$$\underset{\text{advection}}{\frac{\partial}{\partial t}\varepsilon_e + \nabla\cdot(\varepsilon_e \mathbf{v})} + \underset{\text{work}}{p_e \nabla\cdot\mathbf{v}} + \underset{\text{thermal diffusion}}{\nabla\cdot q_t}$$

$$= \underset{\substack{\text{external}\\ \text{heating}}}{W_e} - \underset{\substack{\text{electron/ion}\\ \text{exchange}}}{G - J} + \underset{\substack{\text{current}\\ \text{convection}}}{\mathbf{j}\cdot\nabla\left[\frac{3}{2}\frac{kT_e}{e}\right]} + \underset{\substack{\text{Ohmic}\\ \text{heating}}}{\rho j^2} + \underset{\substack{\text{magnetic}\\ \text{source}}}{\frac{kT_e}{e}\nabla\cdot(\mathbf{j}\cdot\boldsymbol{\beta})}, \tag{4}$$

where the current density

$$\mathbf{j} = \frac{c}{4\pi}\nabla \wedge \mathbf{B} \tag{5}$$

and ε_e, p_e and T_e are the electron energy density, pressure and temperature, respectively. ρ is the plasma resistivity. W_e is the external electron heat deposition rate per unit volume from a source (e.g., a laser). G is the collisional ion/electron heat exchange rate per unit volume, whose value is given by Spitzer [20]. J is an additional ion/electron energy exchange term associated with the work done on the moving fluid by the force resulting from the momentum transfer of the resistance to the electron current flow; its value is given in Ref. [3]. The thermal heat flux is the usual term due to thermal conduction plus a contribution from the thermo-electric effect

$$\mathbf{q}_t = -\boldsymbol{\kappa}_e \cdot \nabla T_e - \{2\beta_{\wedge}(\mathbf{h} \wedge \mathbf{j})kT_e/e\} \tag{6}$$

where **h** is a unit vector in the direction of **B**.

In practice we shall use the specific electron energy (per unit plasma mass), E, as a characteristic variable. This is given by

$$E = \varepsilon_e/d = 3ZkT_e/2m_i = kT_e/\alpha, \tag{7}$$

where d is the plasma density, Z the average ionic charge and m_i the mean ion mass. The constant $\alpha = 2m_i/3Z$. The heavy particle energy density, ε_i, is given by a similar equation, without the magnetic field terms,

$$\underset{\text{advection}}{\partial\varepsilon_i/\partial t + \nabla\cdot(\varepsilon_i\mathbf{v})} + \underset{\text{work}}{p_i\nabla\cdot\mathbf{v}} + \underset{\substack{\text{thermal}\\ \text{conduction}}}{\nabla\cdot\mathbf{q}_i} = \underset{\substack{\text{external}\\ \text{heating}}}{W_i} + \underset{\substack{\text{ion electron}\\ \text{exchange}}}{G + J}, \tag{8}$$

where p_i is the heavy particle partial pressure, $q_i = -\kappa_i \cdot \nabla T$ the heavy particle thermal conduction flux, and W_i the external heavy particle heating rate per unit volume. In this case also we introduce the specific heavy particle energy, $H = \varepsilon_i/d$.

The magnetic field terms also modify the flow velocity via the bulk Lorentz force $\mathbf{j} \wedge \mathbf{B}/c$. Thus Euler's equation becomes:

$$d\left(\frac{\partial \mathbf{v}}{\partial t} + (\mathbf{v} \cdot \nabla)\mathbf{v}\right) = \underset{\substack{\text{magnetic}\\ \text{tension}}}{\frac{1}{4\pi}(\mathbf{B} \cdot \nabla)\mathbf{B}} - \underset{\substack{\text{magnetic}\\ \text{pressure}}}{\frac{1}{8\pi}\nabla(B^2)} - \underset{\substack{\text{particle}\\ \text{pressure}}}{\nabla p}, \tag{9}$$

where p $(= p_i + p_e)$ is the total particle pressure. The generalisation of pressure to a stress tensor is accomplished in the usual way.

The equations are completed by the equation of continuity:

$$\partial d/\partial t + \nabla \cdot (d\mathbf{v}) = 0. \tag{10}$$

We shall use the above equations in these forms. Expressing the derivatives in an appropriate finite difference form, we shall derive difference equations which satisfy the following conservation laws.

(ii) *The Conservation Laws*

Since the flow is hydrodynamic, clearly mass conservation must be satisfied.

Momentum conservation is obtained from Eq. (9) in the usual way.

In order to demonstrate energy conservation we add to equations for ε_e(4) and ε_i(8), the scalar product of (1) with $\mathbf{B}/4\pi$, and the scalar product of (9) with $\mathbf{v}$ to obtain

$$\begin{aligned} &\frac{\partial}{\partial t}(\varepsilon + \tfrac{1}{2}\rho v^2 + B^2/8\pi) + \nabla \cdot [\{\varepsilon + p + \tfrac{1}{2}\rho v^2 + B^2/4\pi\}\mathbf{v}] \\ &\qquad - \nabla \cdot \{(\mathbf{v} \cdot \mathbf{B})B/4\pi\} + \nabla \mathbf{q} + \nabla \cdot (\varepsilon_e v_j) \\ &\quad = W + \frac{1}{4\pi}\nabla \cdot \{[\mathbf{S} - \boldsymbol{\eta} \cdot (\nabla \wedge \mathbf{B})] \wedge \mathbf{B}\}, \end{aligned} \tag{11}$$

where ε is the total thermal energy density $(\varepsilon_e + \varepsilon_i)$; $W = (W_i + W_e)$ is the total external heating rate; $\mathbf{S}$ is in the alternative form [3]

$$\mathbf{S} = c/e\{kT_e \nabla(\ln[n_e]) + \boldsymbol{\beta}^\circ \cdot \nabla(kT_e)\}, \tag{2a}$$

$$\mathbf{q} = \mathbf{q}_t' + \mathbf{q}_i, \tag{12}$$

$\mathbf{q}_t'$ including the complete thermo-electric flux; and $\mathbf{v}_j = -\mathbf{j}/en_e$ is the current velocity.

It is immediately obvious that this equation has a conservative form. However, we note the presence of the fluxes [3] due to the source,

$$\mathbf{Q}_s = -\frac{1}{4\pi}\mathbf{S} \wedge \mathbf{B}, \tag{13}$$

and magnetic diffusion, or Ohmic heating,

$$\mathbf{Q}_\eta = \frac{1}{4\pi}[\boldsymbol{\eta} \cdot (\nabla \wedge \mathbf{B})] \wedge \mathbf{B}. \tag{14}$$

There is one further conservation law obtained from Eq. (1), namely, that for magnetic flux. Thus integrating Eq. (11) over an arbitrary surface with periphery l we obtain

$$\frac{\partial \Phi}{\partial t} + \int_l \mathbf{B} \cdot \mathbf{v} \wedge d\boldsymbol{l} + \int_l (\boldsymbol{\eta} \cdot \nabla \wedge \mathbf{B}) \cdot d\boldsymbol{l} = \int_l \mathbf{S} \cdot d\boldsymbol{l}, \tag{15}$$

where the flux

$$\Phi = \int \mathbf{B} \cdot d\mathbf{s}. \tag{16}$$

Since the integrals in Eq. (15) are all over the bounding line, this clearly yields a conservation law for Φ.

In treating the finite difference form of the Eqs. (1) to (10) it will be important in many cases to ensure that two conservation laws be simultaneously obeyed. In general this well be energy + one other, since all the terms interact in energy. It is therefore convenient to arrange the terms in the equations in complementary pairs which, taken together, mutually maintain energy conservation. Such pairs are:

Eq. (1)	Source	Eq. (4)	Source
Eq. (1)	Diffusion	Eq. (4)	Ohmic heating
Eq. (1)	Advection	Eq. (9)	Magnetic tension and pressure
Eq. (4), Eq. (8)	Work	Eq. (9)	Particle pressure
Eq. (4)	Ion–electron exchange	Eq. (8)	Ion–electron exchange

The algorithms are most naturally developed in these pairs to maintain the conservation laws, and this procedure is adopted here.

Furthermore, some of these terms are standard in that well-known methods are available for their treatment, namely, work/particle pressure in standard hydrodynamical codes [7–10] and ion–electron energy exchange [21]. Although not all such methods exhibit exact conservation we shall assume that some such treatment is used, and therefore we do not consider them further.

3. Conservative Finite Difference Approximations

In view of the conservative form of the preceding equations, it is natural to require that their finite difference representation also obey a conservation relation. Thus consider a closed system (no boundary fluxes) in which the quantities X_l^n generated by the numerical procedure at a mesh point, l, at the conclusion of the nth term step are to be conserved, i.e., $\sum_l X_l^n$ is constant in time. Thus in general for a closed system,

$$\sum_l X_l^n = \sum_l X_l^{n-1} = \cdots = \sum_l X_l^0. \tag{17}$$

We shall call schemes which obey this condition to the accuracy of the round-off error *strongly conservative.*

In many cases the physical quantity, X, is inherently non-negative (e.g., density, energy), in which case the scheme is frequently *non-negativity maintaining*:

$$\text{if } X_l^n \geqslant 0, \text{ then } X_l^{n+1} \geqslant 0 \text{ for all elements, } l. \tag{18}$$

Such a scheme, which is also strongly conservative, obeys the following useful stability theorem:

A non-negativity maintaining, strongly conservative scheme is stable if the input data are non-negative.

The proof follows directly from the definition of stability since any element X_l^n is bounded from above by $\sum_l X_l^0$. The condition on the initial data may be omitted if the scheme is linear and differential (i.e., if $X_l^0 = X_0$, a constant value, then $X_l^n = X_0$), for the system then reduces to an extremal operation of the type considered in Ref. [22].

The strict equality in Eq. (17) may be relaxed to allow an error dependent on the time step Dt of the form

$$\sum_l X_l^n = \sum_l X_l^{(n-1)} + O(Dt^2), \tag{19}$$

which we shall call *weakly conservative.* In contrast to strongly conservative schemes which maintain conservation exactly, weakly conservative schemes may do so to a prescribed accuracy. Thus consider a calculation over a total time $\tau = N\,Dt$ for which

$$\left| \sum_l (X_l^n - X_l^{n-1}) \right| \leqslant K\,Dt^2, \tag{20}$$

where K is a positive real finite number; then the overall conservation error

$$\left| \sum_l (X_l^N - X_l^0) \right| \leqslant NK\,Dt^2 = K\tau\,Dt \tag{21}$$

and may be limited to any value by an appropriate choice of time-step, Dt. In general therefore one introduces an accuracy condition

$$\left| \sum (X_l^{n+1} - X_l^n) \right| \leqslant a \left| \sum X_l^n \right| \tag{22}$$

to limit the conservation error during the calculation, where a is an appropriate fractional error limit.

Such a scheme obeys the important stability theorem:

A non-negativity maintaining, weakly conservative scheme subject to an accuracy condition is stable if the initial data are non-negative.

Suppose there exist a real, positive, finite, constant K such that Eq. (20) is always obeyed; then since the overall error is given by (21), any value X_l^N is bounded from above by $\sum_l X_l^0 + K\tau\, Dt$. The existence of such a constant, K, is ensured by the accuracy condition (22), for if K exists for step $(n-1) \to n$, then $\sum X_l^n$ is bounded. Hence $\sum X_l^{n+1}$ is bounded and K exists for step $n \to (n+1)$. Since $\sum X_l^0$ clearly exists, K exists for step $0 \to 1$, and therefore for all succeeding steps.

A yet weaker form of conservation is

$$\sum_l X_l^n = \sum_l X_l^{(n-1)} + O(Dt), \tag{23}$$

which we call *consistently conservative*. Such schemes cannot improve their conservation accuracy by means of a time-step adjustment.

The above considerations apply to closed systems; however, the extension of these concepts to open systems is straightforward (provided the boundary fluxes are finite) and in no way alters the general results derived.

In this paper we shall only consider strongly and weakly conservative systems, the latter always being assumed subject to an accuracy constraint. In some of the algorithms, the scheme is strongly conservative in one quantity and weakly in a second.

4

(i) *The Mesh and Related Quantities*

We shall consider only cylindrically symmetric systems. For simplicity we assume the mesh has a uniform spacing Δz and δR in the Z and R directions, respectively. Defining the unit vectors $\hat{\mathbf{i}}$ and $\hat{\mathbf{j}}$ in the Z and R directions, respectively, we define the cell corners to be at the points $(i\,\Delta z\,\hat{\mathbf{i}} + j\,\delta R\,\hat{\mathbf{j}})$, where i and j are integers. The cell with corners $\{(i, j), (i+1, j), (i, j+1), (i+1, j+1)\}$ will be called the (i, j) cell. The mesh contains $(IT+1)$ and $(JT+1)$ cells in the Z and R directions, respectively. The axis of symmetry is defined at $j = 0$.

In most Eulerian schemes, the variables are given values at the cell centres $\{(i+\frac{1}{2}), (j+\frac{1}{2})\}$ only. This procedure is adopted throughout in this work, although for some applications the magnetic field (for example) might be more conveniently specified in the centres of the cell faces $\{i, j+\frac{1}{2}\}$ and $\{(i+\frac{1}{2}), j\}$. Thus the fundamental variables of the problem are:

$d_{i+1/2,j+1/2}$	density
$u_{i+1/2,j+1/2}$	Z component of flow velocity
$v_{i+1/2,j+1/2}$	R component of flow velocity
$E_{i+1/2,j+1/2}$	electron specific energy(/unit mass)
$H_{i+1/2,j+1/2}$	heavy particle specific energy
$B_{i+1/2,j+1/2}$	azimuthal magnetic field

Values at points intermediate between cell centres will always be assumed to be obtained by interpolation. Thus,

$$\begin{aligned} X_{i,j+1/2} &= \tfrac{1}{2}(X_{i+1/2,j+1/2} + X_{i-1/2,j+1/2}), \\ X_{i+1/2,j} &= \tfrac{1}{2}(X_{i+1/2,j+1/2} + X_{i+1/2,j-1/2}) \end{aligned} \tag{24}$$

gives the values at the face centres. Values of products at face centres must be taken to be the product of individual terms each centred at the face centre, not the mean of the product terms themselves [17] if the scheme is to be conservative, for example,

$$\begin{aligned} [XY]_{i,j+1/2} &= X_{i,j+1/2}\, Y_{i,j+1/2} \\ &= \tfrac{1}{4}(X_{i+1/2,j+1/2} + X_{i-1/2,j+1/2})(Y_{i+1/2,j+1/2} + Y_{i-1/2,j+1/2}). \end{aligned} \tag{25}$$

In a similar fashion corner values are given by

$$X_{i,j} = \tfrac{1}{4}(X_{i+1/2,j+1/2} + X_{i-1/2,j+1/2} + X_{i-1/2,j-1/2} + X_{i+1/2,j-1/2}). \tag{26}$$

These conventions will be used throughout to denote values obtained for all quantities at points intermediate between cell centres.

The flow variables will be calculated at times $n\,Dt$, where n is integral and Dt the time step, by calculating the time difference $DX^{n+1/2}$ between the values of X at time $(n+1)\,Dt$, X^{n+1}, and at time $n\,Dt$, X^n:

$$DX^{n+1/2} = X^{n+1} - X^n. \tag{27}$$

The superscript thus indicates the time index, n. In the following we shall omit subscripts or superscripts from terms, where their values are obvious or unimportant. Values at intermediate times $(n+\frac{1}{2})\,Dt$ will be defined by interpolation:

$$X^{n+1/2} = \tfrac{1}{2}(X^n + X^{n+1}). \tag{28}$$

In addition to D, the time differencing operator, we also define two space differencing operators, Δ and δ, in the Z and R directions, respectively,

$$\Delta X_{I,J} = X_{I+1/2,J} - X_{I-1/2,J}$$

and (29)

$$\delta X_{I,J} = X_{I,J+1/2} - X_{I,J-1/2},$$

where I, J are arbitrary (integer or half-integer) indices.

In these terms the conservation laws become:

$$\sum_{i,j} D\Phi_{i+1/2,j+1/2} = \text{sum of boundary terms only},$$

$$\sum_{i,j} D\mathscr{E}_{i+1/2,j+1/2} = \text{sum of boundary terms only},$$

where the total flux is given by

$$\Phi_{i+1/2,j+1/2} = \Delta z\, \delta R\, B_{i+1/2,j+1/2} \tag{30}$$

and the total energy by

$$\mathscr{E}_{i+1/2,j+1/2} = V_{j+1/2} \left\{ d_{i+1/2,j+1/2} \left[E_{i+1/2,j+1/2} + H_{i+1/2,j+1/2} + \frac{1}{2} u^2_{i+1/2,j+1/2} + \frac{1}{2} v^2_{i+1/2,j+1/2} \right] + \frac{1}{8\pi} B^2_{i+1/2,j+1/2} \right\}, \tag{31}$$

where $V_{j+1/2}$ is the volume of the cell (i, j).

(ii) *Finite Difference Forms*

In general all the derivatives in Eqs. (1) to (10), with which we shall be concerned, are of one of three types, to each of which we can assign a definite finite difference form to be used throughout this work.

(1) *Time derivatives.*

$$\left[\frac{\partial X}{\partial t}\right]^{n+1/2} \Rightarrow \frac{[DX]^{n+1/2}}{Dt}. \tag{32}$$

(2) ***Second order space derivatives.***

$$\left[\frac{\partial}{\partial z}\left(\alpha \frac{\partial X}{\partial z}\right)\right]_{i+1/2,j+1/2} \Rightarrow [\Delta(\alpha\, \Delta\, X)]_{i+1/2,j+1/2}/\Delta z^2,$$

$$\left[\frac{\partial}{\partial r}\left(\alpha \frac{\partial X}{\partial r}\right)\right]_{i+1/2,j+1/2} \Rightarrow [\delta(\alpha\, \delta\, X)]_{i+1/2,j+1/2}/\delta R^2. \tag{33}$$

(3) *Cross product derivatives.*

$$\left[\frac{\partial}{\partial z}\left(\alpha\frac{\partial X}{\partial r}\right)\right]_{i+1/2,j+1/2} \Rightarrow [\Delta(\alpha\,\delta X)]_{i+1/2,j+1/2}/\Delta z\,\delta R, \tag{34}$$

$$\left[\frac{\partial \alpha}{\partial z}\frac{\partial X}{\partial r}\right]_{i+1/2,j+1/2} \Rightarrow \frac{1}{2}\{[\Delta\,\alpha\,\delta X]_{i+1/2,j+1} + [\Delta\,\alpha\,\delta X]_{i+1/2,j}\}/\Delta z\,\delta R, \tag{35}$$

with similar expressions with z and r interchanged.

In the above expressions X is a general flow variable, and α a general transport coefficient. Some derivatives contain an explicit factor r which is to be taken in the general terms α and X in the expressions above. We shall make strict use of these difference operators, except on the symmetry axis, $j = 0$, where they may be overruled by the rigorous analytic forms (Appendix 1).

Writing out the expressions explicitly by making strict use of the definitions (24) to (29), we see that the derivatives are defined in terms of face-centred quantities $X_{i,j+1/2}$, $X_{i+1/2,j}$, etc., as is necessary for a fully conservative system.

The above definition allows the following derivative equalities to be maintained in finite difference form,

$$\frac{\partial}{\partial z}\left(X\frac{\partial \alpha}{\partial r}\right) - \frac{\partial}{\partial r}\left(X\frac{\partial \alpha}{\partial z}\right)$$

$$\Rightarrow [\Delta(X\,\delta\,\alpha) - \delta(X\,\Delta\,\alpha)]_{i+1/2,j+1/2}/\Delta z\,\delta R \tag{36a}$$

$$= \frac{\partial X}{\partial z}\frac{\partial \alpha}{\partial r} - \frac{\partial X}{\partial r}\frac{\partial \alpha}{\partial z}$$

$$\Rightarrow \frac{1}{2}\begin{bmatrix} [\Delta X \delta\alpha]_{i+1,j+1/2} + [\Delta X \delta\alpha]_{i,j+1/2} \\ -[\delta X \Delta\alpha]_{i+1/2,j+1} - [\delta X \Delta\alpha]_{i+1/2,j} \end{bmatrix} \Big/ \Delta z\,\delta R \tag{36b}$$

$$= \frac{1}{2}\left[\begin{array}{l} \dfrac{\partial}{\partial z}\left(X\dfrac{\partial \alpha}{\partial r}\right) - \dfrac{\partial}{\partial r}\left(X\dfrac{\partial \alpha}{\partial z}\right) \\ \quad + \dfrac{\partial X}{\partial z}\dfrac{\partial \alpha}{\partial r} - \dfrac{\partial X}{\partial r}\dfrac{\partial \alpha}{\partial z} \end{array}\right]$$

$$\Rightarrow \begin{bmatrix} [\delta\alpha]_{i+1,j+1/2} X_{i+3/2,j+1/2} - [\delta\alpha]_{i,j+1/2} X_{i-1/2,j-1/2} \\ -[\Delta\alpha]_{i+1/2,j+1} X_{i+1/2,j+3/2} + [\Delta\alpha]_{i+1/2,j} X_{i+1/2,j-1/2} \end{bmatrix} \Big/ \Delta z\,\delta R, \tag{36c}$$

which follow from

$$\frac{\partial^2 \alpha}{\partial r\,\partial z} = \frac{\partial^2 \alpha}{\partial z\,\partial r} \Rightarrow \delta\Delta\alpha/\Delta z\,\delta R = \Delta\delta\alpha/\Delta z\,\delta R. \tag{37}$$

The above derivative forms occur in all the transport terms. It can be seen that the three are entirely equivalent and the last (36c) is the most compact. For most

purposes it is immaterial which form is used; however, if in the subsequent form alternating direction integration (ADI) is used to integrate the equations it is preferable to use specific forms of (36a), (36b) or (36c) to ensure conservation in each mesh sweep.

In the following sections we shall first give the differential equations, which will then be cast in finite difference form using these relations.

5. The Source Terms

(i) *Finite Difference Approximations*

In cylindrical geometry the source terms in Eqs. (1) and (4) can be written in a number of equivalent forms [3]. For our purposes the most convenient have been found to be

$$\frac{\partial B}{\partial t} = \frac{\alpha c}{e}\left\{\frac{\partial}{\partial r}\left(E\frac{\partial \beta_\perp}{\partial z}\right) - \frac{\partial}{\partial z}\left(E\frac{\partial \beta_\perp}{\partial r}\right) + \frac{\partial}{\partial z}\left(\beta_\wedge \frac{\partial E}{\partial z}\right) + \frac{\partial}{\partial r}\left(\beta_\wedge \frac{\partial E}{\partial r}\right)\right\}, \tag{38}$$

$$\frac{\partial}{\partial t}(\ln E) = \frac{\alpha c}{4\pi e d}\left\{\frac{\partial \beta_\perp}{\partial z}\cdot\frac{1}{r}\frac{\partial}{\partial r}(Br) - \frac{\partial \beta_\perp}{\partial r}\frac{\partial B}{\partial z} - \frac{\partial}{\partial z}\left(\beta_\wedge \frac{\partial B}{\partial z}\right) - \frac{1}{r}\frac{\partial}{\partial r}\left[\beta_\wedge \frac{\partial}{\partial r}(Br)\right]\right\}. \tag{39}$$

Some points may be noted about these equations. The term $E/d(\partial d/\partial t)$ which might be expected from $\partial \varepsilon_e/\partial t$ is included in the energy convection equation. The logarithmic term in (39) is included to maintain positivity of E in the finite difference form of the equation. The asymmetric form of Eqs. (38) and (39) is such that the finite difference approximations to these forms alone maintain energy conservation on each sweep through the mesh.

Using the differencing rules described in Section 4 we obtain

$$B^{n+1}_{i+1/2,j+1/2} = B^n_{i+1/2,j+1/2} + \frac{\alpha c\, Dt}{e} \times \left\{\frac{1}{\Delta z\, \delta R}\left[\delta\{E\Delta\beta_\perp\}_{i+1/2,j+1/2} - \Delta\{E\delta\beta_\perp\}_{i+1/2,j+1/2}\right] + \left[\Delta(\beta_\wedge \Delta E)/\Delta z^2\right]_{i+1/2,j+1/2} + \left[\delta(\beta_\wedge \delta E)/\delta R^2\right]_{i+1/2,j+1/2}\right\} \tag{40}$$

and

$$E^{n+1}_{i+1/2,j+1/2} = E^{n}_{i+1/2,j+1/2} \exp\left\{\frac{\alpha c\, Dt}{4\pi e d_{i+1/2,j+1/2}}\right.$$
$$\times\left[\frac{1}{\Delta z\, \delta R}\left([\Delta\beta_\perp \delta(Br)/r]_{i+1/2,j+1/2} - [\delta\beta_\perp \Delta B]_{i+1/2,j+1/2}\right)\right.$$
$$\left.\left. - \Delta[\beta_\wedge \Delta B/\Delta z^2]_{i+1/2,j+1/2} - [\delta[\beta_\wedge \delta(Br)]/r\, \delta R^2]_{i+1/2,j+1/2}\right]\right\}. \quad (41)$$

Equations (40) and (41) will be shown to be only weakly conservative, but are non-negativity preserving in E, due to the exponential term. A strongly conservative form, but one that is not non-negativity preserving, is obtained by replacing Eq. (41) by the form

$$E^{n+1}_{i+1/2,j+1/2} = E^{n}_{i+1/2,j+1/2} + \frac{\alpha c\, Dt\, E_{i+1/2,j+1/2}}{4\pi e d_{i+1/2,j+1/2}}\left[\frac{1}{\Delta z\, \delta R}\left([\Delta\beta_\perp \delta(Br)/r]_{i+1/2,j+1/2}\right.\right.$$
$$\left. - [\delta\beta_\perp \Delta B]_{i+1/2,j+1/2}\right) - \frac{1}{\Delta z^2}\Delta[\beta_\wedge \Delta B]_{i+1/2,j+1/2}$$
$$\left. - \frac{1}{\delta R^2}[\delta\{\beta_\wedge \delta(Br)\}/r]_{i+1/2,j+1/2}\right]. \quad (41a)$$

We have preferred to maintain energy positivity without a fix and have therefore generally used Eq. (41). Equation (41a) must be treated implicitly in both of the non-linear E, B terms on the right-hand side to maintain stability and its conservative properties. The coupled solution of the pair of Eqs. (40) and (41a) therefore follows the same procedure as that to be described for (40) and (41).

Thus far we have not specified the time values for the terms, B, E, $\beta_\perp$ and $\beta_\wedge$. For second order accuracy in time these should be taken at time $(n+\frac{1}{2})\,DT$ by terms such as

$$B^{n+1/2} = \tfrac{1}{2}(B^{n+1} + B^{n}), \quad (42)$$

i.e., a centred difference form. This, however, requires an implicit treatment of Eqs. (40) and (41). We shall show that the equations above are in fact linearly unstable unless an implicit form is used for B and E with the interpolation parameter, θ, given by

$$B = \theta B^{n+1} + (1-\theta)\, B^{n} \quad (43)$$

in the range $\frac{1}{2} \leq \theta \leq 1$, so that the use of a centred difference or fully implicit scheme

(ii) *Conservative Properties*

It is immediate apparent from Eq. (40) that

$$\sum_{j=0}^{JT}\sum_{i=0}^{IT} DB^{n+1/2}_{i+1/2,j+1/2} = -\frac{ac\,Dt}{e}\left[\sum_{j=0}^{JT}\{[\delta\beta_\perp E]_{IT+1,j+1/2} - [\delta\beta_\perp E]_{0,j+1/2}\}/\Delta z\,\delta R\right.$$
$$+ \{[\beta_\wedge \Delta E]_{IT+1,j+1/2} - [\beta_\wedge \Delta E]_{0,j+1/2}\}/\Delta z^2$$
$$- \sum_{i=0}^{IT}\{[\Delta\beta_\perp E]_{i+1/2,JT+1} - [\Delta\beta_\perp E]_{i+1/2,0}\}/\Delta z\,\delta R$$
$$\left. - \{[\beta_\wedge \delta E]_{i+1/2,JT+1} - [\beta_\wedge \delta E]_{i+1/2,0}\}/\delta R^2\right] \tag{44}$$

and this contains only contributions from the boundaries $i = 0, IT+1, j = 0, JT+1$, in conformity with Eq. (15). It is readily shown that these boundary terms in (44) represent finite difference forms of the integrals in (15).

In order to examine the energy conservation properties of this algorithm we note that

$$DE^{n+1/2} = 2E^{n+1/2}\tanh(De/2) \simeq E^{n+1/2}De\{1 + O(De^2)\}, \tag{45}$$

where De is the argument of the exponential in Eq. (41) and $E^{n+1/2} = \frac{1}{2}(E^n + E^{n+1})$. Neglecting the term in $O(De^3)$ we obtain Eq. (41a). Using the centred difference ($\theta = \frac{1}{2}$) forms of Eqs. (40) and (41a) we obtain, after some algebra,

$$\sum_{j=0}^{JT}\sum_{i=0}^{IT}\left[d_{i+1/2,j+1/2}DE^{n+1/2}_{i+1/2,j+1/2} + \frac{1}{4\pi}B^{n+1/2}_{i+1/2,j+1/2}DB^{n+1/2}_{i+1/2,j+1/2}\right]V_{j+1/2}$$
$$= -\frac{ac\,Dt}{8\pi e}\left\{\sum_{j=0}^{JT} V_{j+1/2}[(\delta\beta_\perp)_{IT+1,j+1/2}[E^{n+1/2}_{IT+3/2,j+1/2}B^{n+1/2}_{IT+1/2,j+1/2}\right.$$
$$+ E^{n+1/2}_{IT+1/2,j+1/2}B^{n+1/2}_{IT+3/2,j+1/2}]$$
$$- (\delta\beta_\perp)_{0,j+1/2}[E^{n+1/2}_{-1/2,j+1/2}B^{n+1/2}_{1/2,j+1/2} + E^{n+1/2}_{1/2,j+1/2}B^{n+1/2}_{-1/2,j+1/2}]]/\Delta z\,\delta R$$
$$- \sum_{i=0}^{IT} S_1\{(\Delta\beta_\perp)_{i+1/2,JT+1}[E^{n+1/2}_{i+1/2,JT+3/2}(Br)^{n+1/2}_{i+1/2,JT+1/2}$$
$$+ E^{n+1/2}_{i+1/2,JT+1/2}(Br)^{n+1/2}_{i+1/2,JT+3/2}]$$
$$\left. - (\Delta\beta_\perp)_{i+1/2,0}[E^{n+1/2}_{i+1/2,1/2}(Br)^{n+1/2}_{i+1/2,-1/2} + E^{n+1/2}_{i+1/2,-1/2}(Br)^{n+1/2}_{i+1/2,1/2}]/\Delta z\,\delta R\}\right\}$$
$$+ \frac{ac\,Dt}{4\pi e}\left\{\sum_{j=0}^{JT} V_{j+1/2}[\beta_{\wedge IT+1,j+1/2}\{B^{n+1/2}_{IT+1/2,j+1/2}\Delta E^{n+1/2}_{IT+1,j+1/2}\right.$$
$$\left. - E^{n+1/2}_{IT+1/2,j+1/2}\Delta B^{n+1/2}_{IT+1,j+1/2}\}\right.$$

$$-\beta_{\wedge 0,j+1/2}\{B^{n+1/2}_{1/2,j+1/2}\Delta E^{n+1/2}_{0,j+1/2} - E^{n+1/2}_{1/2,j+1/2}\Delta B^{n+1/2}_{0,j+1/2}\}]/\Delta z^2$$
$$+\sum_{i=0}^{IT} S_1\,\beta_{\wedge i+1/2,JT+1}\{(Br)^{n+1/2}_{i+1/2,JT+1/2}\delta E^{n+1/2}_{i+1/2,JT+1}$$
$$-E^{n+1/2}_{i+1/2,JT+1/2}\delta(Br)_{i+1/2,JT+1}\}/\delta R^2\Big\}, \tag{46}$$

where the cell volume $V_{j+1/2} = S_1 r_{j+1/2}$. In deriving these terms we have made use of the fact that since B vanishes on the axis, $\beta_{\wedge i+1/2,0} = 0$.

We observe from this result that these are only contributions from the bounding surfaces, and that in consequence the algorithm is conservative. Furthermore, if reflective boundary conditions are used to define $E_{IT+3/2,j+1/2}$, etc. (see Eq. (123)), the finite differences give a good approximation to the source flux $\mathbf{Q}_s$ in Eq. (13). There is one serious defect, namely, the existence of a flux across the cylindrical axis. So far, however, we have not defined the terms $E_{i+1/2,-1/2}$ and $(Br)_{i+1/2,-1/2}$. We may therefore choose their values to give a zero flux across the axis, namely,

$$E_{i+1/2,-1/2} = E_{i+1/2,1/2} : (Br)_{i+1/2,-1/2} = -(Br)_{i+1/2,1/2}. \tag{47}$$

At first sight this choice for $(Br)_{i+1/2,-1/2}$ may appear inconsistent with the symmetry relation for B (Appendix 1). However, within the finite difference scheme it is used to calculate $(Br)_{i+1/2,0} = \frac{1}{2}[(Br)_{i+1/2,1/2} + (Br)_{i+1/2,-1/2}] = 0$, and is therefore correct for the application for which it is used. For other applications—such as to directly calculate the derivative—a different interpretation of $(Br)_{i+1/2,-1/2}$ may be necessary; indeed with this value the algorithm does not exactly reproduce the known analytic solution [3]. The actual choice made will depend on the weight assigned to the integral as opposed to differential properties of the model. In our opinion it is best to maintain the conservation laws since the value of the parameter is always to be regarded as some form of average over the cell. Equation (47) does not represent the only possible choice for $E_{i+1/2,-1/2}$ and $(Br)_{i+1/2,-1/2}$, but is the best one consistent with a reasonable definition of the axial current from equation (5) and has therefore been adopted for use in the code MAGT.

In the case of energy conservation time ordering is important. Centred difference schemes give overall energy conservation accurate to the order of $O(Dt^3)$ at worst. Fully implicit (or explicit) schemes will be conservative only to terms $O(Dt^2)$.

(iii) *Stability*

It was shown in Ref. [3] that the coupled source equations admit wave-like solutions. Furthermore it is well-known [23] that the wave equation gives stability problems in finite difference form, particularly if the amplitude and its derivative are both evaluated at the cell centre, when simple explicit algorithms are absolutely unstable. This unstable behaviour was observed in practice with an early code using an explicit solution to the magnetic field problem; study of these stability problems

led to the identification of thermal magnetic waves [3], and to the algorithms presented here.

The stability of the finite difference forms, Eqs. (40) and (41) is, however, unconditionally established through the conservation relation (46) and the non-negativity maintaining nature of Eq. (41). It is clear that since even the explicit form is weakly conservative in energy the forms are stable independent of the implicitness parameter, θ. This does not, however, imply that all forms are well-behaved. Thus let us consider the linearised stability analysis for the case $\beta_{\wedge} = 0$, $\partial\beta_{\perp}/\partial z = 0$ and $\partial\beta_{\perp}/\partial r = \text{const.}$, where the algorithm has the simple form

$$\begin{aligned} B_{I,J}^{n+1} &= B_{I,J}^{n} - \frac{1}{2}\frac{\alpha c}{e}\frac{Dt}{\Delta z}\frac{\delta\beta_{\perp}}{\delta r} \\ &\quad \times \{E_{I+1,J}^{n+1}\theta + E_{I+1,J}^{n}(1-\theta) - E_{I-1,J}^{n+1}\theta - E_{I-1,J}^{n}(1-\theta)\} \\ E_{I,J}^{n+1} &= E_{I,J}^{n} - \frac{1}{2}\frac{\alpha c\, Dt}{4\pi d_{I,J} e}\frac{\delta\beta_{\perp}}{\Delta z\, \delta r}\{E_{I,J}^{n+1}\theta + E_{I,J}^{n}(1-\theta)\} \\ &\quad \times \{B_{I+1,J}^{n+1}\theta + B_{I+1,J}^{n}(1-\theta) - B_{I-1,J}^{n+1}\theta - B_{I-1,J}^{n}(1-\theta)\}. \end{aligned} \tag{48}$$

Considering an error of the usual form in both B and E, namely, $be^{il\Delta z}$ and $\Sigma e^{il\Delta z}$, respectively, we obtain a growth constant

$$\gamma = \frac{b^{n+1}}{b^{n}} = \frac{\Sigma^{n+1}}{\Sigma^{n}} \tag{49}$$

given by

$$\begin{aligned} &(\gamma - 1)(\gamma - E_{I,J}^{n+1}/E_{I,J}^{n}) \\ &\quad = \frac{E_{I,J}^{n}}{4\pi d_{I,J}} \cdot \left(\frac{\alpha c}{e}\frac{\delta\beta_{\perp}}{\delta R}\right)^{2}\left(\frac{Dt}{\Delta z}\right)^{2}(\gamma\theta + (1-\theta))^{2}\sin^{2}(k\,\Delta z). \end{aligned} \tag{50}$$

This is simplified if $E_{I,J}^{n+1}/E_{I,J}^{n} \simeq 1$ to

$$\gamma = \frac{1 \pm i(1-\theta)\,\Gamma_0}{1 \mp i\theta\Gamma_0}, \tag{51}$$

where

$$\Gamma_0 = \sqrt{\frac{E_{I,J}^{n}}{4\pi d_{I,J}}}\left(\frac{\alpha c}{e}\right) \cdot \frac{\delta\beta_{\perp}}{\delta r} \cdot \frac{Dt}{\Delta z}\sin(k\Delta z).$$

This linearised form of the algorithm is only stable if $|\gamma| \leqslant 1$, i.e., if $\theta \geqslant \frac{1}{2}$. Examination of Eq. (48) shows that the origin of this instability can be traced to a failure of Eq. (48) to maintain $E_{i,j}$ non-negative. Furthermore we note that in this

simple form the algorithm is non-dispersive if $\theta = \frac{1}{2}$. This is behaviour is demonstrated in Fig. 1, where a thermal magnetic wave solution is shown calculated with the non-negativity maintaining algorithm (41) for values of $\theta = 0, \frac{1}{2}$ and 1 in the special case where $\beta_\perp = \beta_\perp(z)$, and is discussed more fully in section 5(iv). Phase and amplitude error are introduced by the fully implicit solution ($\theta = 1$), but the centred difference scheme faithfully reproduces the analytic form. An explicit calculation ($\theta = 0$) shows increasing growth as predicted by (51).

Thus explicit forms of (40) and (41), whilst not strictly unstable in the sense that growth is unbounded, are unsatisfactory in that they exhibit a large, but bounded, growth of these error terms, the amplitude of the errors being limited to the magnitude of the quantities themselves. A similar calculation can be performed for the z derivatives, with similar results. Thus we conclude that the terms $\beta_\perp$ are only treated satisfactorily if $\theta \geqslant \frac{1}{2}$. In an ADI calculation the growth is due to an explicit step of $Dt/2$ and an implicit step of $Dt/2$, the net growth constant

$$\gamma' = \frac{1 + i\Gamma_0}{1 - i\Gamma_0} \tag{52}$$

and $|\gamma'|^2 = 1$.

We must now examine the behaviour of the terms containing $\beta_\wedge$. It follows from the stability theorem outlined earlier that these terms are also strictly stable. However, as before this does not imply that the algorithm is satisfactory. We consider first the linearised form of Eqs. (40) and (41) with $\beta_\perp = 0$, $\beta_\wedge = \text{const}$ and variations of B and E in z only. For this case, also, we obtain the growth constant γ given by Eq. (51) but with Γ_0 replaced by

$$\Gamma_1 = 2\frac{\alpha c}{e}\beta_\wedge \sqrt{\frac{E^n_{I,J}}{4\pi d_{I,J}}}\frac{Dt}{\Delta z^2}\left[1 - \cos(k\,\Delta z)\right] \tag{53}$$

and conclude that the terms B and E must also be treated with $\theta \gtrsim \frac{1}{2}$.

There is a further complication with regard to the term $\beta_\wedge$, whose numerator is linearly proportional to B [18]. Thus Eq. (40) contains terms of the form

$$\frac{\partial B}{\partial t} = \frac{\alpha c}{e}\beta'_\wedge \frac{\partial E}{\partial z}\frac{\partial B}{\partial z} + \cdots, \tag{54}$$

i.e., an advection term with speed $-(\alpha c/e)\beta'_\wedge(\partial E/\partial z)$, where $\beta'_\wedge = \beta_\wedge/B$.

This term is differenced explicitly in time, and by centred difference (in B) in space, which by a classic result is linearly unstable [23] and therefore unsatisfactory. To resolve this difficulty is straightforward by pursuing the hydrodynamic analogy. Thus we may retain the spatial centred difference and treat the term in B in Eq. (54)

implicitly within the Newton–Raphson iteration. Alternatively we may use upstream differencing for $\partial B/\partial z$ in either an implicit or explicit form:

$$\beta_{\wedge I+1/2,J} = \beta'_{\wedge I+1/2,J} \begin{cases} B_{I+1,J} & \text{if} \quad (\beta'_{\wedge}\partial E/\partial z)_{I+1/2,J} > 0 \\ B_{I,J} & \text{otherwise.} \end{cases} \tag{55}$$

Of these alternatives implicit centred differencing suffers from the possibility that a solution to the implicit equation in B may not exist. The upstream differencing approach, however, avoids this difficulty, and is therefore used in the code MAGT. Experience has indicated that the explicit form is simpler to code, and runs satisfactorily. A time-step constraint of the usual form in advection (Eq. (90)) is necessary to avoid a spurious change in sign of B due to term (54). We note that the conservation properties are not changed by the form of $\beta_{\wedge}$ adopted, since the finite difference schemes (40) and (41) are conservative on each sweep through the mesh.

(iv) *Numerical Tests*

In view of the complicated structure of he governing equations, no analytic solutions of the complete set of equations are known. Some useful similarity solutions to the source equations (38) and (39) in one dimension exist [3] and these will be used to examine the behaviour of the finite difference approximations (40) and (41) to these equations. These solutions exist only for the case where $\beta_{\wedge} = 0$.

The first such solution reveals the existence of thermal magnetic waves. Thus consider a plasma of ambient electron energy, E_0, and zero field, with $\beta_{\perp}$ a function of r only. Then there exists a perturbation solution

$$B = B_1 \exp\{i(\omega t - kz)\} : E = E_1 \exp\{i(\omega t - kz)\} \tag{56}$$

corresponding to a wave propagating in the z direction with frequency

$$\omega = \sqrt{\frac{E_0}{4\pi d}} \cdot \alpha \frac{d\beta_{\perp}}{dr} \cdot k. \tag{57}$$

We have already, in Section 5(iii), investigated the response of the linearised algorithm to this wave, and found that the wave is only well described by a centred difference approximation, amplitude and phase errors being introduced by other forms of time differencing.

A more sensitive test of the spatial and temporal differencing is provided by the case $\beta_{\perp} = \beta_{\perp}(z)$ only, where the waves are cylindrical. It is shown in Ref. [3] that in this case the waves are described by Bessel functions, with a standing wave distribution

$$E = E_1 J_0(kr) \cos\ \omega t : B = B_1 J_1(kr) \sin \omega t \tag{58}$$

with

$$B_1 = -\sqrt{\left\{\frac{4\pi d}{E_0}\right\}} E_1. \tag{59}$$

Figure 1 shows the response of the full algorithm to this problem. An energy perturbation of amplitude 10^{-4} units is applied to a plasma of mean energy 1 unit, with no initial magnetic field. The plasma length of 12 mesh cells is taken to be one full wavelength of the perturbation. The magnetic field B is zero at the end of the mesh, and the electron energy, E, is oscillated at the frequency, ω, corresponding to the wavelength through Eq. (57) at the boundary. A standing wave is therefore established on the mesh, described approximately by the Bessel function distribution (58). Figure 1 shows the temporal behaviour of the magnetic field and electron energy in cell 6 near the first maximum of the electron energy and a zero of the magnetic

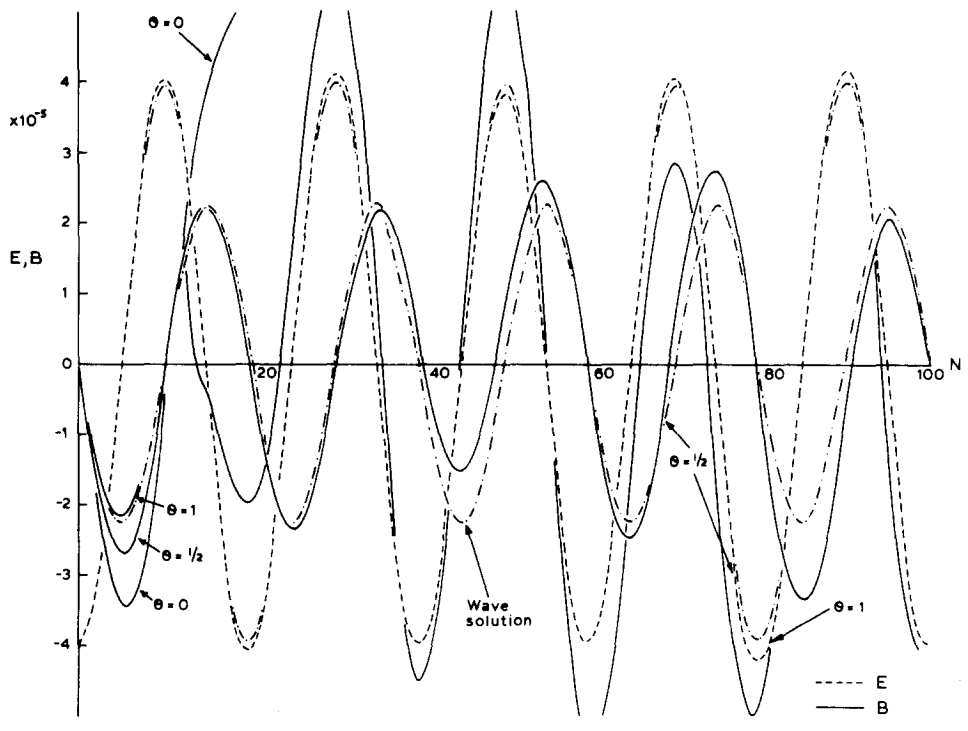

a

FIG. 1. Comparison of numerical and analytic solutions of the radial thermal magnetic wave problem described in the text, Section 5(iv). The variation of magnetic field (B) (solid line) and specific electron energy (E) (dashed line) as functions of the number of integration steps (N) are shown in (a) for explicit ($\theta = 0$), centred difference ($\theta = \frac{1}{2}$) and implicit ($\theta = 1$) forms of the positivity maintaining finite difference term. The exact perturbation solution (chain line) is also shown, clearly distinguished by its constant amplitude. The unstable behaviour of the explicit form is shown in (b), where the peaks of the magnetic field (O) and electron energy (X) are plotted logarithmically against the integration step (N).

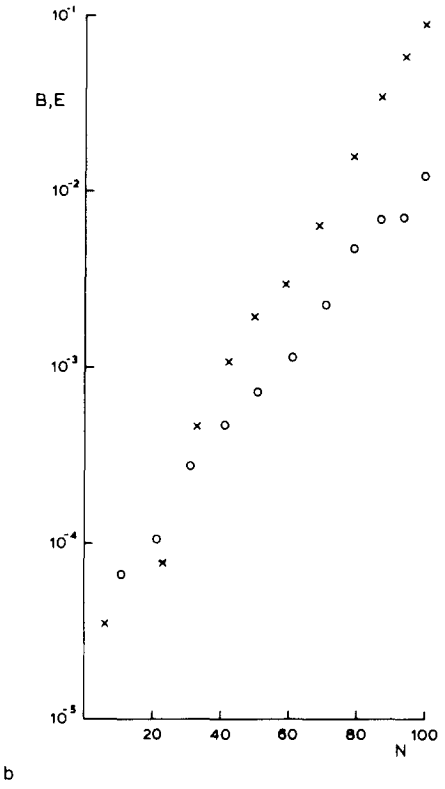

b

FIG. 1—*Continued.*

field. The time step used was 1/20 of the period ($\omega\, Dt \simeq 0.31416$). As can be seen from Fig. 1 the centred difference scheme gives a reasonably accurate representation of this wave: a detailed study of the numerical results shows that after 100 time-steps the maximum amplitude error from the exact solution is less than 1%.

The inaccuracy of the coarse spatial differencing (12 cells/wavelength), and the inexact differencing of the Bessel function are reflected in the errors introduced into the values of the magnetic field, B. The electron energy being calculated at its maximum is relatively accurately spatially determined, and its errors therefore essentially represent temporal differencing inaccuracy. Nonetheless the error in B is always relatively small, less than 10% of the amplitude, and no spatial phase errors occur with centred differencing.

In contrast both explicit and implicit differencing are unsatisfactory. As can be seen from Fig. 1b, the explicit calculation shows an unstable exponential growth with number of steps as predicted by the linear analysis; the growth, however, is eventually limited by the non-negativity condition and weak conservative form but only at values comparable with the ambient conditions. The implicit calculation shows large phase and amplitude error. In particular we note the behaviour after about 12 time-steps where the field at cell 6 shows a rapid decrease. This is associated with a wave

which propagates from the origin and reflects the inability of this solution to match the boundary conditions at the origin. (Note that since these waves are dispersion free the wave takes $\sim\frac{1}{2}$ period to propagate $\sim\frac{1}{2}$ wavelength.)

A second problem for which analytic solutions exist is provided by the one dimensional case where $\beta_\perp$ is a function of r only and

$$B = -\sqrt{4\pi d E_0}\, z f(x) : E = E_0 z^2 g(x) \tag{60}$$

where

$$x = \frac{\alpha c}{e}\frac{d\beta_\perp}{dr}\sqrt{E_0/4\pi d}\, t. \tag{61}$$

The analytic solutions are

$$f(x) = 2\tan(x) : g(x) = \sec^2 x. \tag{62}$$

Inserting these forms in the spatial differences of Eqs. (40) and (41) we find that the numerical scheme reproduces solutions (60) but with f and g given by

$$f^{n+1} = f^n - 2(\theta g^{n+1} + (1-\theta)\, g^n)\, Dx :$$
$$g^{n+1} = g^n \exp\{-(\theta f^{n+1} + (1-\theta) f^n)\, Dx\}, \tag{63}$$

demonstrating the second order spatial differencing accuracy. It is clear from Eq. (62) that these solutions represent a phase of rapid growth of the magnetic field and electron energy. The accuracy of the numerically generated solutions f^n and g^n may be directly assessed against the known exact forms, and provides a sensitive test of the temporal integration procedure.

We may examine the existence of solutions of Eq. (63). Eliminating f^{n+1} we obtain

$$g^{n+1} = g^n \exp\{-[f^n - 2\theta(1-\theta)\, g^n\, Dx]\, Dx\} \exp\{2\theta^2 g^{n+1}\, Dx^2\}. \tag{64}$$

Consider the behaviour of the function

$$y = x - \alpha e^{\beta x} \tag{65}$$

for which $y \to -\infty$ as $x \to \pm\infty$ and which has a single maximum of value $1/\beta\{\ln(1/\alpha\beta) - 1\}$ at $x = 1/\beta \ln(1/\alpha\beta)$. Real solutions of Eq. (64) therefore only exist if

$$2\theta^2 g^n \exp\{1 - [f^n - 2\theta(1-\theta)\, g^n\, Dx]\, Dx\}\, Dx^2 \leqslant 1 \tag{66}$$

and the smallest such solution gives the most accurate approximation. For a fully implicit calculation ($\theta = 1$) this restricts the initial step-length $Dx \leqslant \sqrt{2/e} \simeq 0.43$ and for a centred difference ($\theta = \frac{1}{2}$), $Dx \lesssim \frac{3}{4}$. For an explicit calculation ($\theta = 0$) there is no restriction of the step-length. The origin of this difficulty is readily seen from Eq. (63) to be due to the non-linear term g in the equation for g^{n+1} and occurs if any implcit

form for E is taken on the right hand side of Eq. (41). In practice this implies no additional restriction of the algorithm (40)/(41) provided the integration step-length is controlled to obey physical constraints satisfactorily.

The physical origin of this absence of a solution is clearly seen in the exact solution (62) for which a solution only exists if $x \leqslant \pi/2$. In a similar fashion the finite difference form only exhibits solutions for restricted times, Dx.

Figure 2a shows a comparison of the implicit, explicit and centred difference schemes for a calculation with $Dx = 0.1$. The failure of the implicit form after 10

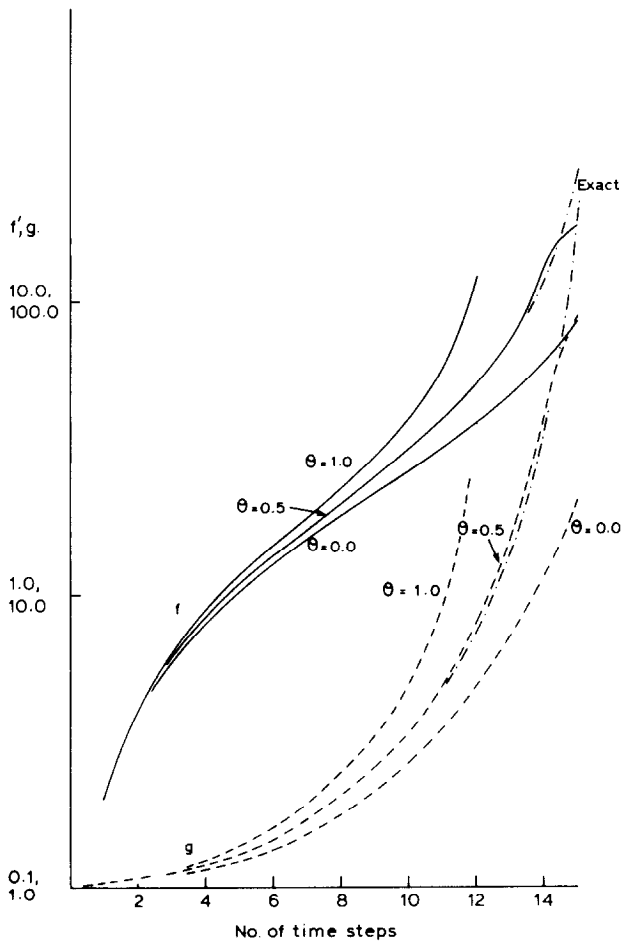

a

FIG. 2. Comparison of the numerical and analytic solutions of the similarity grwoth problem described in the text, Section 5(iv). The variation of the variables f and g as functions of the number of time steps are shown in (a) for explicit ($\theta = 0$), centred difference ($\theta = \frac{1}{2}$) and implicit ($\theta = 1$) forms. The variation of error with integration step-length is shown in (b) for both magnetic field ($\oplus, \otimes$) and electron energy ($+, \times$) at time 1.0 using explicit and centred difference forms. The straight lines show the expected first order and second order error variations of the respective forms.

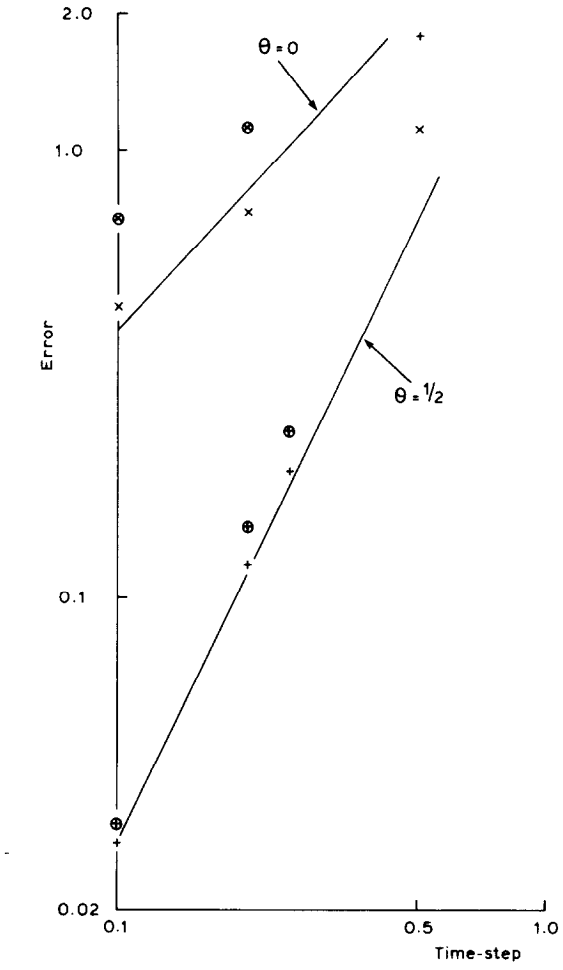

FIG. 2—*Continued.*

time-steps can be seen. The marked improvement in accuracy obtained by using the centred difference is most noticeable. In Fig. 2b we examine the variation in error with step-length. It can be seen that for the explicit term, the error varies as Dx, being first order, whereas the centred difference error shows second order Dx^2 dependence. A reasonable level of error for the second order term is obtained with $Dx \lesssim 0.25$.

(v) *Alternating Direction Integration*

The preceding analysis of the conservation and stability properties of the finite difference forms, Eqs. (40) and (41), indicate that a centred difference form should be used.

The two dimensional form of the equations is a further complication. However,

fortunately in one dimension the equations may be cast into a generalised tri-diagonal form, which may be solved by a generalisation of the standard recursion routine [23, p. 277]. The equations are thus well suited to the application of the standard ADI [24, 25] scheme particularly in view of the fact that in most practical applications the problem is dominated by a density gradient in one dimension (Z), i.e., is one dimensionally dominant. However, it is worth noting that the asymmetric ICCG method [18] can also be used for this problem.

Equations (40) and (41) are non-linear both by virtue of the dependence of the transport coefficients $\beta_\perp$ and $\beta_\wedge$ on B and E, and the explicit exponential term. In principle we could treat the complete non-linearity within the following iterative procedure. In practice since the field free coefficient in $\beta_\perp$ is independent of E, and field dependent contributions from $\beta_\perp$ and $\beta'_\wedge$ depend on B^2 and higher terms, we have found it satisfactory to calculate $\beta_\perp$ and $\beta'_\wedge$ at the start of the time-step ($n\,Dt$) only, and use these values explicitly. The non-linearities due to the argument of the exponential only are solved iteratively. The nature of these non-linearities, in particular the exponential form, make the problem extremely suitable for solution by a Newton–Raphson technique, which will rapidly converge, provided such a solution exists.

The algorithm thus proceeds as follows:

Sweep 1. Calculate approximate values of $\tilde{B}^{n+1/2}$ and $\tilde{E}^{n+1/2}$ from Eqs. (40) and (41) using B^n and E^n on the right hand side, with time interval $\frac{1}{2}Dt^{n+1/2}$. Newton–Raphson iterate in one direction (say, Z) to obtain the ADI values at the intermediate time $\bar{B}^{n+1/2}$ and $\bar{E}^{n+1/2}$.

Sweep 2. Calculate approximate values of $\tilde{B}^{n+1}$ and $\tilde{E}^{n+1}$ from (40) and (41) using $\bar{B}^{n+1/2}$ and $\bar{E}^{n+1/2}$. Newton–Raphson iterate in the other direction (R) to obtain B^{n+1} and E^{n+1}.

Since the operations in the directions R and Z do not commute, as a consequence of the spatially varying coefficients and the exponential term, the routine is clearly not symmetric in R and Z. Approximate symmetry, however, may be introduced by alternating the order of the direction of the sweeps 1 and 2 as the routine proceeds.

(vi) *The Newton–Raphson Iteration*

The Newton–Raphson iteration is performed as follows. Consider the z-differencing term over an interval DT, which may be written in the form

$$\begin{aligned} B_{I,J} &= B^0_{I,J} + AX_{I,J}E_{I+1,J} - BX_{I,J}E_{I,J} + CX_{I,J}E_{I-1,J}, \\ E_{I,J} &= E^0_{I,J} \exp\{AY_{I,J}B_{I+1,J} - BY_{I,J}B_{I,J} + CY_{I,J}B_{I-1,J}\}, \end{aligned} \tag{67}$$

where $I = i + \frac{1}{2}$, $J = j + \frac{1}{2}$, and $B^0_{I,J}$ and $E^0_{I,J}$ are the values of $B_{I,J}$ and $E_{I,J}$ on entry to the implicit stage. The arrays $AX \cdots CY$ are given by

$$AX_{I,J} = -\frac{\alpha c}{e} DT \left\{ \frac{1}{2} \delta\beta_{\perp I+1/2,J}/\Delta z\, \delta R - \beta_{\wedge I+1/2,J}/\Delta z^2 \right\},$$

$$
\begin{aligned}
BX_{I,J} &= -\frac{\alpha c\, DT}{e}\left\{\frac{1}{2}(\delta\beta_{\perp I+1/2,J}-\delta\beta_{\perp I-1/2,J})/\Delta z\,\delta R\right.\\
&\qquad\left.-(\beta_{\wedge I+1/2,J}+\beta_{\wedge I-1/2,J})/\Delta z^2\right\},\\
CX_{I,J} &= \frac{\alpha c\, DT}{e}\left\{\frac{1}{2}\delta\beta_{\perp I-1/2,J}/\Delta z\,\Delta R+\beta_{\wedge I-1/2,J}/\Delta z^2\right\},\\
AY_{I,J} &= -\frac{\alpha c\, DT}{4\pi d_{I,J}e}\left\{\frac{1}{2}\delta\beta_{\perp I+1/2,J}/\Delta z\,\delta R+\beta_{\wedge I+1/2,J}/\Delta z^2\right\},\\
BY_{I,J} &= -\frac{\alpha c\, DT}{4\pi d_{I,J}e}\left\{\frac{1}{2}(\delta\beta_{\perp I+1/2,J}-\delta\beta_{\perp I-1/2,J})/\Delta z\,\delta R\right.\\
&\qquad\left.+(\beta_{\wedge I+1/2,J}+\beta_{\wedge I-1/2,J})/\Delta z^2\right\},\\
CY_{I,J} &= \frac{\alpha c\, DT}{4\pi d_{I,J}e}\left\{\frac{1}{2}\delta\beta_{\perp I-1/2,J}/\Delta z\,\delta R-\beta_{\wedge I-1/2,J}/\Delta z^2\right\}.
\end{aligned}
\tag{68}
$$

These equations are to be solved by iteration. Thus if $\tilde{B}_{I,J}$ and $\tilde{E}_{I,J}$ are given by the previous iteration, the next set of values are given by

$$
\begin{aligned}
B_{I,J} &= \tilde{B}_{I,J}+\delta B_{I,J},\\
E_{I,J} &= \tilde{E}_{I,J}+\delta E_{I,J},
\end{aligned}
\tag{69}
$$

where $\delta B_{I,J}$ and $\delta E_{I,J}$ are solutions of

$$\delta B_{I,J}-AX_{I,J}\,\delta E_{I+1,J}+BX_{I,J}\,\delta E_{I,J}-CX_{I-1,J}\,\delta E_{I,J}=DX_{I,J}, \tag{70}$$

$$\delta E_{I,J}-AY'_{I,J}\,\delta B_{I+1,J}+BY'_{I,J}\,\delta B_{I,J}-CY'_{I,J}\,\delta B_{I-1,J}=DY_{I,J}. \tag{71}$$

If $\bar{B}_{I,J}$ and $\bar{E}_{I,J}$ are the values of $B_{I,J}$ and $E_{I,J}$ obtained from (67) with $\tilde{E}_{I,J}$ and $\tilde{B}_{I,J}$ on the right hand side,

$$DX_{I,J}=\bar{B}_{I,J}-\tilde{B}_{I,J};\qquad DY_{I,J}=\bar{E}_{I,J}-\tilde{E}_{I,J} \tag{72}$$

and

$$AY'_{I,J}=\bar{E}_{I,J}AY_{I,J},\quad BY'_{I,J}=\bar{E}_{I,J}BY_{I,J},\quad CY'_{I,J}=\bar{E}_{I,J}CY_{I,J}. \tag{73}$$

A simple recursive algorithm for solving general tridiagonal equations of the type (70), (71) is given in Ref. [23, p. 277].

It is easily shown that the calculation in the R direction is cast into a similar form.

Most ADI forms are only weakly conservative due to the non-linearity in E and B

in Eqs. (41) and (41a). Resulting from the fact that the increase in magnetic energy between two time levels 0 and 1,

$$(B^{12} - B^{02})/8\pi = B^{1/2}\, DB^{1/2}/4\pi, \tag{74}$$

a strongly conservative scheme must be centre differenced in B on the right hand side of (41a) and the unsuperscripted terms $E_{i+1/2,j+1/2}$ be taken at the same time in both (40) and (41a). Since Eqs. (40) and (41a) in this form conserve energy exactly on each sweep through the mesh, the ADI form with sweeps of the following form is strongly conservative.

Sweep 1, explicit in R and implicit in Z, consists of the operations:

$$\begin{aligned}
\tilde{B}^{n+1/2} &= B^n + \frac{1}{2}\frac{\alpha c\, Dt}{e}\{\delta[E^n\, \Delta\beta_\perp]/\Delta z\, \delta R + \delta[\beta_\wedge\, \delta E^n]/\delta R^2\},\\
\tilde{E}^{n+1/2} &= E^n + \frac{1}{2}\frac{\alpha c\, Dt}{4\pi e d} E^n\{\Delta\beta_\perp\, \delta(\bar{B}^n r)/r\, \Delta z\, \delta R - \delta[\beta_\wedge\, \delta(\bar{B}^n r)]/r\, \delta R^2\},\\
B^{n+1/2} &= \tilde{B}^{n+1/2} - \frac{1}{2}\frac{\alpha c\, Dt}{e}\{\Delta[E^{n+1/2}\, \delta\beta_\perp]/\Delta z\, \delta R - \Delta[\beta_\wedge\, \Delta E^{n+1/2}]/\Delta z^2\},\\
E^{n+1/2} &= \tilde{E}^{n+1/2} - \frac{1}{2}\frac{\alpha c\, Dt}{4\pi e d} E^{n+1/2}\{\delta\beta_\perp \Delta\bar{B}^{n+1/2}/\Delta z\, \delta R + \Delta[\beta_\wedge \Delta\bar{B}^{n+1/2}]/\Delta z^2\},
\end{aligned} \tag{75}$$

where

$$\bar{B}^v = \frac{1}{2}(B^v + \tilde{B}^{n+1/2}). \tag{76}$$

Sweep 2, explicit in Z and implicit in R, is constructed in a similar fashion. Provided the terms are calculated in the order shown, the evaluation of the terms $\tilde{B}^{n+1/2}$ for use in $\tilde{E}^{n+1/2}$ is accomplished without recourse to elimination. This solution is unconditionally linearly stable.

In principle, since the algorithm is absolutely stable, one would expect that it may be used with any step-length. Such a procedure does not, however, ensure the existence of a solution of the Newton–Raphson iteration, as in Eq. (63). Let us examine the condition that the solution to Eq. (67) exists. We may write the general form of Eq. (67) as

$$E_k = E_k^0 \exp\left\{\sum_l Y_{kl} B_l^0 + \sum_{l,m} Y_{kl} X_{lm} E_m\right\}, \tag{77}$$

where k, l, m are general indices (I, J) and X and Y are the tridiagonal matrices (CX, BX, AX) and (CY, BY, AY), respectively. Clearly a solution to Eq. (77) only exists if

$$\operatorname*{Min}_{E_k'} \frac{E_k^0}{E_k'} \exp\left\{\sum_l Y_{kl} B_l^0 + \sum_{l,m} Y_{kl} X_{lm} E_m'\right\} \leqslant 1, \tag{78}$$

where E'_m is the set of values E_m with E_k replaced by E'_k. Since the minimum of $1/xe^x$ occurs at $x = 1$, the value of E'_k generating the minimum is

$$E'_k = 1 \Big/ \sum_l Y_{kl} X_{lk} \tag{79}$$

and the solution exists if $E'_k \leqslant 0$ or

$$\sum_l Y_{kl} B^0_l + \sum_l Y_{kl} X_{lm} E'_m \leqslant \ln(E'_k/E^0_k). \tag{80}$$

Since the matrix elements X and Y are proportional to the time-step DT, this condition is clearly established by a suitable choice of the time-step. For if the argument of the exponent is made small, Eq. (80) yields

$$\sum_l Y_{kl} B^0_l + \sum_{l,m} Y_{kl} X_{lm} E'_m \leqslant 1 \Big/ \sum_l Y_{kl} X_{lk} E^0_k - 1, \tag{81}$$

a condition established if

$$\sum_l Y_k X_k E^0_k = (A Y_k C X_{k+1} + B Y_k B X_k + C Y_k A X_{k-1}) E^0_k \ll 1. \tag{82}$$

Since this condition essentially limits the change in electron energy allowed in any time-step, it will be subsequently seen to be necessary on physical grounds. Due to the fact that the overall condition (80) is established in the course of the iterative calculation it is possible that a failure to converge may ocur, although in the author's experience with this routine when the step-length has been determined by Eq. (89) this has never happened. A simple remedy to alleviate this problem, should it arise, whilst incurring a minimum of error is to allow E_k to take the limit value E'_k in the iteration. In particular, if $\bar{E}_{I,J}$ in Eqs. (72) and (73) is replaced by $E'_{I,J}$ and $AY_{I,J}$, $CY_{I,J}$ set to zero and $BY_{I,J}$ set to unity the iteration will converge on to the limit value. A simple test for this condition is [illegible] the argument of the exponential,

$$De' = \sum_l Y_{kl} B_l, \tag{83}$$

and inequality (80) therefore may be written

$$De' + \{1 - E_k/E'_k\} \lesssim \ln(E'_k/E^0_k). \tag{84}$$

Similar problems are also introduced if the alternative form (41a) is used, which again reduce to a condition of the form (81) namely,

$$\left\{1 - \left(\sum_l Y_{kl} B^0_l + \frac{1}{2} \sum_{\substack{l,m \\ m \neq i}} Y_{kl} X_{lm} E_m\right)\right\}^2 \geqslant 2 \sum_l Y_{kl} X_{lk} E^0_k, \tag{81a}$$

which yields a condition of the same form as that of (82). The test equivalent to (84) is

$$\{(1 - E_k/E'_k) - De'\}^2 \gtrsim 2E^0_k/E'_k. \tag{84a}$$

(vii) *Time-Step Constraints*

Although the algorithm is absolutely stable, and can in principle be used with any arbitrary time-step, we have seen that solutions of the implicit form only exist under restricted conditions. In practice this result is the mathematical expression of the physical behaviour we observed in our test solutions in Fig. 2. Thus in the example of Fig. 2 the exact solution only exists for times

$$t < \frac{\pi}{2} \Big/ \left\{ \frac{\alpha c}{e} \frac{|\nabla \beta_\perp|}{l} \sqrt{\frac{E}{4\pi d}} \right\}, \tag{85}$$

where l is a characteristic length.

Similarly the thermal magnetic wave solutions of Fig. 1 also show behaviour with a characteristic time,

$$\tau = \left\{ \frac{\alpha c}{e} \frac{|\nabla \beta_\perp|}{l} \sqrt{\frac{E}{2\pi d}} \right\}^{-1}. \tag{86}$$

For a satisfactory treatment of either of these effects the time-step $Dt \ll \tau$. Indeed Fig. 2b indicates that a value of order $Dt \approx 0.1\tau$ should be used to ensure accuracy of about 1%.

In a similar fashion Eq. (53) indicates that the presence of wave solutions associated with the cross product terms $\beta_\wedge$. Including these the characteristic time

$$\tau = \left\{ \frac{\alpha c}{e} \sqrt{\frac{E}{2\pi d}} \left[\frac{|\nabla \beta_\perp|}{l} + \frac{|\beta_\wedge|}{l^2} \right] \right\}^{-1}. \tag{87}$$

Since we wish, in practice, to resolve effects over a few mesh spacings the characteristic length must be taken to be the smallest of Δz and δR:

$$l = \mathrm{Min}(\Delta z, \delta R). \tag{88}$$

With this choice of l we have found a satisfactory time-step to be

$$Dt \leqslant 0.25\tau, \tag{89}$$

a value which is also compatible with condition (82).

The truncation error terms in Eqs. (40) and (41), which govern the energy conservation error in the weak algorithm, also depend essentially on the ratio Dt/τ. Thus if a conservation error limit is included, this also provides a separate restriction on Dt. We shall discuss this limit below, in the section dealing with the complete code.

The "advection" term (54) introduces a time-step constraint associated with its physical nature. The term $\beta_\wedge$ has the limit $\beta_\wedge \to 0$ as $B \to 0$, so that the term (54) cannot of itself change the sign of B. This behaviour is avoided if the upstream differencing of B in Eq. (55) is made subject to the time-step constraint

$$Dt \leqslant 1 \Big/ \frac{\alpha c}{e} \{\beta'_\wedge \operatorname{Max}[|\Delta E|/\Delta z^2, |\delta E|/\delta R^2]\}. \tag{90}$$

6

(i) *Magnetic Diffusion–Ohmic Heating*

In cylindrical geometry the magnetic diffusion term yields

$$\frac{\partial B}{\partial t} = \frac{\partial}{\partial z}\left[\eta_\perp \frac{\partial B}{\partial z}\right] + \frac{\partial}{\partial r}\left[\frac{\eta_\perp}{r}\frac{\partial}{\partial r}(Br)\right] + \frac{\partial}{\partial r}\left(\frac{\eta_\wedge}{r}\right)\frac{\partial}{\partial z}(Br) - \frac{\partial}{\partial z}\left(\frac{\eta_\wedge}{r}\right)\frac{\partial}{\partial r}(Br) \tag{91}$$

and the Ohmic heating rate per unit volume,

$$\frac{\partial w}{\partial t} = \frac{1}{4\pi}\eta_\perp\left[\left(\frac{\partial B}{\partial z}\right)^2 + \left(\frac{1}{r}\frac{\partial}{\partial r}(Br)\right)^2\right]. \tag{92}$$

We note there is no contribution of $\eta_\wedge$ to the Ohmic heating.

The treatment of the derivatives in Eq. (91) is straightforward using the general rules (33)–(36) yielding the finite difference form

$$\begin{aligned} B^{n+1}_{i+1/2,j+1/2} = B^n_{i+1/2,j+1/2} &+ Dt\{\Delta[\eta_\perp \Delta B]_{i+1/2,j+1/2}/\Delta z^2 \\ &+ \delta[\eta_\perp/r\,\delta(Br)]_{i+1/2,j+1/2}/\delta R^2 \\ &+ \{\delta[\eta_\wedge \Delta B]_{i+1/2,j+1/2} - \Delta[\eta_\wedge/r\,\delta(Br)]_{i+1/2,j+1/2}\}/\Delta z\,\delta R\} \end{aligned} \tag{93}$$

except adjacent to the axis in the cells $j = 0$, where the term $\delta[\eta_\perp/r\,\delta(Br)]$ is undefined. To avoid this defect we put

$$\begin{aligned} &\frac{\partial}{\partial r}\left[\frac{\eta_\perp}{r}\frac{\partial}{\partial r}(Br)\right]_{i+1/2,1/2} \\ &\quad \Rightarrow \frac{1}{\delta R^2}\left[\frac{\eta_\perp}{r}\delta(Br)\right]_{i+1/2,1} - \frac{1}{\delta R}\left[\eta_\perp\left[\frac{1}{r}\frac{\partial}{\partial r}(Br)\right]^D\right]_{i+1/2,0}, \end{aligned} \tag{94}$$

where the superscript D is to indicate its use with the diffusion. The limit

$$\lim_{r\to 0} \frac{1}{r}\frac{\partial}{\partial r}(Br)$$

is, of course, finite and finite difference forms based on analytic forms near the axis are given in Appendix 1. In fact the conservation properties determine which form is appropriate to use (see Eq. (100)).

In a similar fashion we use finite difference equation (66) to give the Ohmic heating in time Dt per unit volume:

$$w_{i+1/2,j+1/2} = \frac{Dt}{8\pi}\{(\eta_{\perp i+1,j+1/2}[\Delta B]^2_{i+1,j+1/2} + \eta_{\perp i,j+1/2}[\Delta B]^2_{i,j+1/2})/\Delta z^2$$
$$+ (\eta_{\perp i+1/2,j+1}[\delta(Br)/r]^2_{i+1/2,j+1} + \eta_{\perp i+1/2,j}[\delta(Br)/r]^2_{i+1/2,j})/\delta R^2\}. \tag{95}$$

As with Eq. (91) we note that the terms in the cell $j = \frac{1}{2}$ will again "blow up." To avoid this we put

$$\frac{1}{\delta R}\left[\frac{1}{r}\delta(Br)\right]_{i+1/2,0} \Rightarrow \left[\frac{1}{r}\frac{\partial}{\partial r}(Br)\right]^{H}_{i+1/2,0}, \tag{96}$$

where the H indicates that it is associated with the heating term. The value given to this derivative will also be determined by energy conservation considerations (Eq. (101)).

The complete finite difference form of the magnetic diffusion is a typical diffusion equation, although the cross product $\eta_\wedge$ terms introduce asymmetry. As with all such equations it is only unconditionally stable in a centred difference or fully implicit form (see Section 6(ii)). As we shall show, only the centred difference form is fully conservative. We may, however, prefer to relax this condition and treat diffusion as a stiff process, with an arbitrary time-step, in which case the fully implicit form is to be preferred as it does not introduce spurious reversals of sign: the difficulties introduced by this stiff form from the cross product terms will be considered in Appendix 2. The implicit equation can be solved by one of the standard methods, ADI or preferably asymmetric ICCG [18], the latter being used in MAGT.

(ii) *Conservative Properties*

Consider first the conservation of flux:

$$\sum DB_{i+1/2,j+1/2} = Dt\sum_j \Bigg[\{[\eta_\perp \Delta B]_{IT+1,j+1/2} - [\eta_\perp \Delta B]_{0,j+1/2}\}/\Delta z^2$$
$$+ \frac{1}{2}\left\{\delta\left[\frac{\eta_\wedge}{r}\right]_{IT+1,j+1/2}[(Br)_{IT+3/2,j+1/2} + (Br)_{IT+1/2,j+1/2}]\right.$$

$$- \delta \left[\frac{\eta_\wedge}{r}\right]_{0,j+1/2} [(Br)_{-1/2,j+1/2} + (Br)_{1/2,j+1/2}] \Big\} \Big/ \Delta z\, \delta R \Big]$$

$$+ Dt \sum_i \Big[\Big\{ \left[\frac{\eta_\perp}{r} \delta(Br)\right]_{i+1/2,JT+1} / \delta R - \left[\frac{\eta_\perp}{r}\left[\frac{\partial}{\partial r}(Br)\right]^D\right]_{i+1/2,0} \Big\} \Big/ \delta R$$

$$- \frac{1}{2} \Big\{ \left[\frac{\eta_\wedge}{r}\right]_{i+1/2,JT+1} [(Br)_{i+1/2,JT+3/2} + (Br)_{i+1/2,JT+1/2}] \Big\} \Big/ \delta R\, \Delta z \Big]. \tag{97}$$

The conservation of energy yields

$$\sum_{i,j} [w_{i+1/2,j+1/2} + B^{n+1/2}_{i+1/2,j+1/2}\, DB_{i+1/2,j+1/2}/4\pi]\, V_{j+1/2}$$

$$= \frac{Dt}{4\pi} \Big\{ \sum_j \Big[V_{j+1/2} ([\eta_\perp B\, \Delta B]_{IT+1,j+1/2} - [\eta_\perp B\, \Delta B]_{0,j+1/2}) / \Delta z^2$$

$$+ \frac{1}{2} S_1 \left(\delta \left(\frac{\eta_\wedge}{r}\right)_{IT+1,j+1/2} (Br)_{IT+1/2,j+1/2} (Br)_{IT+1,j+1/2} \right.$$

$$\left. - \delta \left(\frac{\eta_\wedge}{r}\right)_{0,j+1/2} (Br)_{1/2,j+1/2} (Br)_{1/2,j+1/2} \right) \Big/ \Delta z\, \delta R \Big]$$

$$+ \sum_i \Big[\frac{V_{JT+1/2} r_{JT+3/2}}{r^2_{JT+1}} [\eta_\perp B \delta(Br)]_{i+1/2,JT+1} / \delta R^2$$

$$- V_{1/2} \eta_{\perp i+1/2,0} \Big[\Big[\frac{1}{r} \frac{\partial}{\partial r} (Br) \Big]^{H^2}_{i+1/2,0} - 2B_{i+1/2,1/2} \Big[\frac{1}{r} \frac{\partial}{\partial r} (Br) \Big]^D_{i+1/2,0} \Big/ \delta R \Big]$$

$$- \frac{1}{2} S_1 \Delta \left(\frac{\eta_\wedge}{r}\right)_{i+1/2,JT+1} (Br)_{i+1/2,JT+1/2} (Br)_{i+1/2,JT+3/2} / \Delta z\, \delta R \Big] \Big\}. \tag{98}$$

Clearly there is no flux on axis so that these terms must satisfy

$$\Big[\frac{1}{r} \frac{\partial}{\partial r} (Br) \Big]^{H^2}_{i+1/2,0} = 2B_{i+1/2,1/2} \Big[\frac{1}{r} \frac{\partial}{\partial r} (Br) \Big]^D_{i+1/2,0} \Big/ \delta R. \tag{99}$$

A suitable form given in Appendix 1 is

$$\Big[\frac{1}{r} \frac{\partial}{\partial r} (Br) \Big]^D_{i+1/2,0} = 4B_{i+1/2,1/2} / \delta R, \tag{100}$$

giving

$$\Big[\frac{1}{r} \frac{\partial}{\partial r} (Br) \Big]^H_{i+1/2,0} = 2\sqrt{2}\, B_{i+1/2,1/2} / \delta R. \tag{101}$$

If these forms are used the energy generated by Ohmic heating is consistent with the depletion of magnetic energy. The apparent inconsistency in Eqs. (100) and (101) is not significant, and is due to the implicit assumption that the same value of B can be used to give a good approximation to both B and B^2 within a cell. The inclusion of the differences (100) and (101) in Eqs. (93) and (95) are mutually consistent, viewed in terms of cell averaged quantities.

Since the term $B^{n+1/2}_{i+1/2,j+1/2}$ on the left-hand side of Eq. (98) is defined at time $(n+\frac{1}{2})\,Dt$, Eq. (98) is only exact if all the terms on the right-hand side involving this term are taken at this time. This may be achieved by writing the squares in the Ohmic heating expression (95) in the form of products of differences taken at two different time levels, e.g.,

$$[\Delta B]^2 \Rightarrow [\Delta B]^{n+1/2}[\Delta B]^{\nu}, \tag{102}$$

where ν is the time level of B on the right-hand side of Eq. (93). Only in this centred difference form do Eqs. (93) and (95) yield exact energy conservation, i.e., are strongly energy conservative. Alternative forms, which may be preferable for other reasons, are only weakly conservative. In this connection it is perhaps of interest to note the similarity of this scheme to that of Christiansen and Roberts [26], working on a non-uniform one dimensional mesh. The generalisation of the above forms to a non-uniform mesh is readily accomplished by the following modified terms in Eqs. (93) and (95), the remaining terms being unchanged. We consider the case of non-uniform space in Z, the case of a variable mesh in R being treated in an identical fashion. The modified terms in (93) are

$$B^{n+1}_{i+1/2,j+1/2} = B^{n}_{i+1/2,j+1/2} + Dt\,\Delta[\eta_{\perp}\,\Delta B/\Delta z]_{i+1/2,j+1/2}/\Delta z_{i+1/2}. \tag{103}$$

However, we note that in forming the difference form (95) the Ohmic heating is calculated in terms of quantities evaluated for pseudo-cells whose centres lie at the cell face centres. Since we clearly add the contributions from each pseudo-cell to give a total for the real cell corresponding to the volume overlap, we obtain, for the modified form of (95),

$$w_{i+1/2,j+1/2} = \frac{Dt}{8\pi}\left\{\frac{\Delta z_{i+1}}{\Delta z_{i+1/2}}\cdot\eta_{\perp i+1}[\Delta B/\Delta z]^2_{i+1,j+1/2} + \frac{\Delta z_i}{\Delta z_{i+1/2}}\,\eta_{\perp i}[\Delta B/\Delta z]^2_{i,j+1/2}\right\} + \cdots. \tag{104}$$

It is readily shown that this form is exactly conservative if centred diffeencing is used. The generalisation to consider non-uniformity in R is accomplished in an identical fashion.

We may now identify the scheme with that of Ref. [26]. In that work the algorithm is defined in terms of the electric field and the current density, which in our scheme are defined at the cell faces, and the Ohmic heating calculated within a cell of Δz_{i+1}

spacing about that point, i.e., within the psuedo-cell used to derive Eq. (104). The method of Ref. [26] applied to present problem reduces to a calculation on a pair of de-coupled meshes (i) and $(i+\frac{1}{2})$ with B defined on one mesh and (E, j) on the other. In the present method of calculating Ohmic heating is thus equivalent to a calculation on one of the meshes only, and in this form is identical to that of Ref. [26]. The centred difference criterion for exact energy conservation is equivalent to that of Ref. [26], namely, that the electric field term, $\Delta B^{n+1/2}$, must be time centred and the current taken at the same time as in diffusion, $\eta[\Delta B]^*$. In this connection we may note the considerable reduction in storage and work obtained by avoiding the need to evaluate the pair of two component vectors at each mesh point.

7

(i) *Thermal Energy Diffusion*

In these terms we consider the individually energy conservative terms involving electron thermal conduction, current convection and the residual thermo-electric flux. The governing differential equation can be reduced to

$$\frac{\partial E}{\partial t} = \frac{\partial}{\partial z}\left(\chi_\perp \frac{\partial E}{\partial z}\right) + \frac{1}{r}\frac{\partial}{\partial r}\left(r\chi_\perp \frac{\partial E}{\partial r}\right) + \frac{1}{r}\left[\frac{\partial}{\partial r}(r\chi'_\wedge)\frac{\partial E}{\partial z} - \frac{\partial (r\chi'_\wedge)}{\partial z}\frac{\partial E}{\partial r}\right] + \frac{\alpha c}{4\pi e d}\left\{\frac{1}{r}\frac{\partial}{\partial r}\left[2\beta_\wedge E \frac{\partial}{\partial r}(Br)\right] + \frac{\partial}{\partial z}\left[2\beta_\wedge E \frac{\partial B}{\partial z}\right]\right\}. \tag{105}$$

We have included the current convection with the cross product heat conduction (Righi–Leduc) term by introducing the coefficients

$$\chi_\perp = \alpha\kappa_\perp/k : \chi'_\wedge = \alpha(\kappa_\wedge/k + cB/4\pi e), \tag{106}$$

where $\kappa_\perp$ and $\kappa_\wedge$ are the coefficients of electron thermal conduction.

This equation is readily put into finite difference form using (33) to (36) to give an equation of the usual form for diffusion, but asymmetric due to the cross product terms, namely,

$$E^{n+1}_{i+1/2,j+1/2} = E^n_{i+1/2,j+1/2} + Dt\left[\Delta[\chi_\perp \Delta E]_{i+1/2,j+1/2}/\Delta z^2 + \left[\frac{1}{r}\delta\{r\chi_\perp \delta E\}\right]_{i+1/2,j+1/2}\Big/\delta R^2 + \frac{1}{2}\frac{1}{r_{j+1/2}}\{[\Delta E\,\delta(r\chi'_\wedge)]_{i+1,j+1/2} + [\Delta E\,\delta(r\chi'_\wedge)]_{i,j+1/2}\right.$$

$$- [\delta E\, \Delta(r\chi'_{\wedge})]_{i+1/2,j+1} - [\delta E\, \Delta(r\chi'_{\wedge})]_{i+1/2,j}\}/\Delta z\, \delta R$$
$$+ \frac{2\alpha c}{4\pi e d_{i+1/2,j+1/2}} \left\{ \frac{1}{r_{j+1/2}} \delta[\beta_{\wedge} E\, \delta(Br)]_{i+1/2,j+1/2}/\delta R^2 \right.$$
$$\left. + \Delta[\beta_{\wedge} E\, \Delta B]_{i+1/2,j+1/2}/\Delta z^2 \right\} \Bigg]. \tag{107}$$

Although these terms do not significantly change the general method, they can cause the introduction of spurious changes of sign unless care is taken to prevent this (Appendix 2). As is well known, the simple diffusion equation must be solved implicitly [23] if it is to be unconditionally stable. The subsequent analysis will show that this condition remains unchanged by the cross product terms. Thus (107) should be integrated by some implicit method, ADI, or better, asymmetric ICCG [18], the latter being used in MAGT.

The finite difference form of (107) is obviously conservative, by virtue of the forms of the differences used.

The cross product terms can be differenced in a slightly different manner, whilst remaining conservative,

$$\frac{1}{r}\frac{\partial}{\partial r}(r\chi'_{\wedge})\frac{\partial E}{\partial z} - \frac{\partial \chi'_{\wedge}}{\partial z}\frac{\partial E}{\partial r} \Rightarrow \left[\frac{1}{r}\delta(r\chi'_{\wedge})\Delta E - \Delta\chi'_{\wedge}\,\delta E\right]_{i+1/2,j+1/2} \Big/ \Delta z\, \delta R \tag{108}$$

instead of form (36). This term, however, introduces problems with the axial cell $\{i, 0\}$, particularly when the equations are used in a stiff form. Although these problems can be satisfactorily overcome, they are best avoided by the use of face-centred differencing—form (36), where $(r\chi'_{\wedge})_{i+1/2,0} = 0$ is explicitly used.

(ii) *Stability*

The stability behaviour of the linearised form of Eq. (107) without the cross product terms is well-known [21]. In this section we simply extend this result in the usual way be considering the growth of an error in E of the form $\Sigma^n e^{ilk\Delta z}$. In one dimension the finite difference equation with constant coefficients has the form

$$E_l^{n+1} = E_l^n + \alpha_1(\tilde{E}_{l+1} - 2\tilde{E}_l + \tilde{E}_{l-1}) + \alpha_2(\tilde{E}_{l+1} - \tilde{E}_{l-1}), \tag{109}$$

where

$$E_l = \theta E_l^{n+1} + (1-\theta)\, E_l^n. \tag{110}$$

Hence the growth rate of the error, $\gamma = \Sigma^{n+1}/\Sigma^n$ is given by

$$= \frac{1 - \Gamma(1-\theta)}{1 + \Gamma\theta}, \tag{111}$$

where $\Gamma = 2\{\alpha_1[1 - \cos(k\,\Delta z)] + i\alpha_2 \sin(k\,\Delta z)\}$.

The stability condition $|\gamma|^2 \leqslant 1$ is satisfied if

$$2\theta - 1 \geqslant -\frac{\alpha_1[1-\cos(k\,\Delta z)]}{\alpha_1^2[1-\cos(k\,\Delta z)]^2 + \alpha_2^2 \sin^2[k\,\Delta z\,]}, \tag{112}$$

which yields a condition on θ,

$$\theta \geqslant \frac{1}{2} - \frac{1}{2}\frac{\alpha_1}{\alpha_1^2 + \alpha_2^2 + [\alpha_1^2 - \alpha_2^2]}; \tag{113}$$

i.e., if $\theta \geqslant \frac{1}{2}$, as for the normal case.

This conclusion is readily extended to include two dimensional diffusion processes. We also note that these results apply to magnetic diffusion described by (93).

8

(i) *Magnetic Stress/Advection*

In this case the complementary terms are the Lorentz force terms in Euler's equation,

$$d\frac{\partial u}{\partial t} = -\frac{1}{8\pi}\frac{\partial}{\partial z}(B^2), \tag{114}$$

$$d\frac{\partial v}{\partial t} = -\frac{1}{4\pi}\frac{B^2}{r} - \frac{1}{8\pi}\frac{\partial}{\partial r}(B^2), \tag{115}$$

and the advection term,

$$\frac{\partial B}{\partial t} = -\frac{\partial}{\partial z}(uB) - \frac{\partial}{\partial r}(vB). \tag{116}$$

The latter equation is identical to the usual continuity equation in two dimensional Cartesian (as opposed to cylindrical) co-ordinates. As is well known this term is troublesome [23], but several well-behaved methods [7–10] are available and it is assumed that one of these is used here, presumably the same scheme as that used for the hydrodynamics. The magnetic pressure may then be treated in a similar fashion to the particle pressure. It then remains only to find a conservative prescription for the Maxwell tension term. The actual form we use will depend on the form of radial pressure differencing used. Thus if we use face-centred differencing [8]

$$\frac{\partial}{\partial r}(B^2)\bigg|_{i+1/2,j+1/2} \Rightarrow \frac{1}{2}\left\{\frac{r_{j+1}[\delta(B)^2]_{i+1/2,j+1} + r_j[\delta(B)^2]_{i+1/2,j}}{r_{j+1/2}}\right\}\Big/\delta R \tag{117}$$

we use a face-centred form of B^2

$$\frac{B^2}{r}\bigg|_{i+1/2,j+1/2} \Rightarrow \frac{1}{2}\frac{[(B)_{i+1/2,j+1}]^2 + [(B)_{i+1/2,j}]^2}{r_{j+1/2}}. \tag{118}$$

Or in direct difference form [7],

$$\frac{\partial}{\partial r}(B^2)\bigg|_{i+1/2,j+1/2} \Rightarrow \frac{1}{2}\{(B^2)_{i+1/2,j+3/2} - (B^2)_{i+1/2,j+1/2}\}/\delta R \tag{119}$$

and

$$\frac{B^2}{r}\bigg|_{i+1/2,j+1/2} \Rightarrow \frac{1}{2}\frac{[B_{i+1/2,j+3/2}B_{i+1/2,j+1} + B_{i+1/2,j}B_{i+1/2,j+1/2}]}{r_{j+1/2}}. \tag{120}$$

It is easily shown that the contribution of these two terms is identical from both prescriptions.

(ii) *Conservative Properties*

It is clear that in any well-chosen hydrodynamic scheme both axial momentum and flux will be conserved. The radial momentum is conserved trivially in cylindrical geometry. It therefore remains only to consider energy conservation.

In a typical second order hydrodynamic scheme the advection typically has the form

$$DB_{i+1/2,j+1/2} = -\frac{Dt}{\Delta z}[\Delta(uB)]_{i+1/2,j+1/2} - \frac{Dt}{\delta R}[\delta(vB)]_{i+1/2,j+1/2}. \tag{121}$$

We may remark that no algorithm can use this term and be stable; however, most schemes obey this equation to terms $O(Dt^2)$ at least. Hence,

$$\begin{aligned}
&\sum [V\{d[u\,Du + v\,Dv] + B^{n+1/2}\,DB/4\pi\}]_{i+1/2,j+1/2} \\
&\quad = \frac{Dt}{\Delta z}\sum_j V_{j+1/2}\{[u_{-1/2,j+1/2}B_{1/2,j+1/2} + u_{1/2,j+1/2}B_{-1/2,j+1/2}]\,B_{0,j+1/2} \\
&\qquad - [u_{IT+3/2,j+1/2}B_{IT+1/2,j+1/2} + u_{IT+1/2}B_{IT+3/2,j+1/2}]\,B_{IT+1,j+1/2}\}/8\pi \\
&\qquad - \frac{Dt}{\delta R}\sum_i S_1\{v_{i+1/2,JT+1/2}(rB)_{i+1/2,JT+3/2} \\
&\qquad + v_{i+1/2,JT+3/2}(rB)_{i+1/2,JT+1/2}\}\,B_{i+1/2,JT+1}/8\pi.
\end{aligned} \tag{122}$$

This result obtained using either (117) or (119) is clearly conservative. It also has the desirable property that there is no axial flux on axis if $B_{i+1/2,0} = 0$, as it should be on physical grounds.

9. Boundary Conditions

Thus far we have described algorithms which generate numerical approximations to the differential equations in the bulk. In an attempt to model a physical problem we must clearly specify boundary conditions to our numerical problem which are compatible with those of the physical case. The mathematical structure of the underlying physical equations (hyperbolic or parabolic) demands that the boundary conditions be those of an initial value problem, namely, that the physical parameters (d, u, v, E, H, B) be specified throughout the mesh at the initial instant of time, and that Dirichlet or Neumann boundary conditions be applied at the spatial boundaries at all times.

The first of these conditions, namely, the initial state, will depend on the problem considered by the user. In typical laser plasma interaction modelling it will consist of a uniform slab target, adjacent to a "vacuum" interface. The only difficulty introduced by this case is that within an Eulerian scheme, as described here, all cells must have a non-zero density and it is therefore necessary to introduce a progressive density decrease in the "vacuum" zone.

At the spatial boundaries we may specify either the value or the normal derivative. In practice for the types of problems treated by these codes these boundaries take one of two forms:

(a) *Reflective.* It is assumed that at a reflective boundary the physical quantity is uniform across the boundary, for example,

$$X_{IT+3/2,j} = X_{IT+1/2,j}. \tag{123}$$

The normal derivative across a reflective boundary is zero and any diffusive flux across it therefore zero. It is therefore also called a closed boundary.

(b) *Open.* The value of the physical quantity is set at some specified value.

$$X_{IT+3/2,j} = \text{specified value}. \tag{124}$$

In general the algorithms described here are designed to be used with either form of boundary condition. In the code MAGT the boundary conditions are entirely reflective, with one exception. The application of these values is straightforward except for the case of the magnetic field, where the radial condition

$$(Br)_{i,JT+3/2} = (Br)_{i,JT+1/2}. \tag{125}$$

is used to satisfy Ampère's law.

The use of reflective boundary conditions conforms to the known conditions of the physical problems in all cases but one—magnetic diffusion. In this case the magnetic field will diffuse across the boundary into the undisturbed slab material, or the field lines penetrate into the vacuum region propagating as a low frequency electromagnetic wave. The exact boundary conditions at the edge of the mesh are therefore unknown. The practical alternatives at our disposal, namely, a reflective boundary or an open one with boundary value set to zero, represent opposite extreme approx-

imations—the first allowing no flux to cross the boundary, the second coercing the maximum transfer. In an effort to find an intermediate condition, we have considered the following approximation. The normal computational mesh is enclosed by a single layer of boundary cells. The outer boundary of these boundary cells is made reflective (closed). At the start of each magnetic diffusion calculation the field in the boundary cells is set to zero, and flux allowed to diffuse into these cells across the mesh boundary, to the limit allowed by the implicit calculation. The diffused flux in the cells is then assumed to rapidly decay, and be lost to the mesh. In most cases the effects of magnetic diffusion across the boundary are negligibly small.

The use of reflective boundary conditions in E and B in the source algorithms implies a non-zero energy flux across the boundary (46), which is the numerical form of the flux (13) and is associated with the Poynting vector of the electro-magnetic field due to the electric field induced along the boundary by the pressure gradient and the azimuthal magnetic field. The existence of an energy source/sink is thus implied in the region adjacent to the boundary, whose temperature and density match that within the mesh.

As discussed earlier it is advantageous to use the split-time step philosophy and separate the various calculations into their complementary parts. In this way a strongly conservative scheme can be generated if the appropriate centred difference implicit schemes are used, together with an exactly energy conserving hydrodynamic term. In practice the latter may present problems due to the need to treat the advection of the complete energy term from which must be subtracted electron, magnetic and kinetic energies to determine the ion thermal energy. The overall conservation error may, however, be limited by a time-step constraint as in Section 3, if the system is weakly conservative. Thus if the total energy in the mesh is $\mathscr{E}^n$ and the conservation error for step n is $D\mathscr{E}^n$ we may restrict the time-step for step $(n+1)$

$$Dt^{n+1} = a\mathscr{E}^n/D\mathscr{E}^n \cdot Dt^n. \tag{126}$$

The order in which the operations are performed in a split-time step scheme is only unimportant if the operations involved all commute. One can readily show that except for the case of constant coefficients, none of the operations described in Sections 5–7 do commute, and one must take account of the ordering of steps in the code. A reasonable sequence, bearing in mind the physical effect of each operation, is

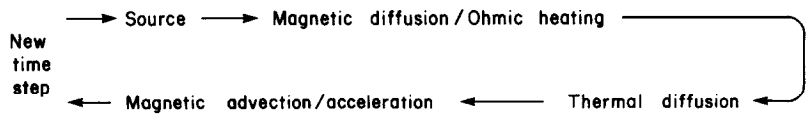

and is used in the code MAGT.

The code MAGT has been constructed using the algorithms described earlier. The hydrodynamics are solved by donor cell differencing with anti-diffusion flux correction (FCT) [8, 10]. This method is effectively of second order accuracy, and is used in weakly conservative form for the pressure work/kinetic energy terms. The model considers two temperatures, electron and ion, whose equilibration is solved by a positivity maintaining routine [27], similar to that described in Ref. [21]. The programme is designed to study the interaction of laser radiation with a solid target considered as an ideal gas and models the absorption of the laser beam via inverse bremsstrahlung and a reflective dump at the critical density to provide an electron heat source. The transport coefficients used are given by Braginskii [19], with standard flux limitation [28] plus options for ion-acoustic flux limitation and Bohm diffusion. The code is in two versions using either the non-negativity preserving, but weakly conservative, source algorithm, Eq. (41), or the strongly conservative form (41a) with a fix-up. A continuous energy balance, allowing for the fluxes out of the mesh, is evaluated, and the conservation error used to limit the time-step Dt, through Eq. (26). The accuracy factor, a, used for time-step limitation is the same as that used to determine the accuracy of the solutions in the ICCG and Newton–Raphson solutions. There is thus a conservation error resulting from the iteration error, which is of the same order of magnitude as that which results from the truncation error of the finite difference schemes. Experience indicates that for reasonable values of the accuracy parameter, the step-length is usually controlled by other limits in the programme, namely, the Courant–Fredrichs–Lewy condition, the source conditions (89) or (90), diffusion accuracy limits or a limit on the energy deposition in a cell within one time-step.

We have found that using these algorithms it is not necessary to include either artificial smoothing [14] in addition to that introduced by the FCT algorithm or any reset to zero (except as noted in the conservative form). The solutions generated by these finite difference forms maintain essential positivity, and are well behaved, with no rapid variations in space or time, provided the various limiting conditions indicated in the paper are observed.

11. Test Runs

We present some results obtained with the code MAGT to illustrate various features of the computational scheme. Since we are concerned with the numerical behaviour of the code rather than the physical nature of this interaction process we shall consider the calculation for a fixed set of input data. The mesh used had cell dimensions $(\Delta z, \delta R) = (2.5, 10)\,\mu$m and contained 30×10 cells, the latter being smaller than is generally used for modelling studies. The target was solid carbon, assumed to have an average charge of 5, with an initial temperature of 10^4 K. The solid initially occupied 7 cells in the Z direction, the density then decreasing by a factor of 4 from cell to cell outwards up to cell 16, and remaining constant thereafter at a value equal to 10^{-4} of the critical density: the initial density was uniform in R.

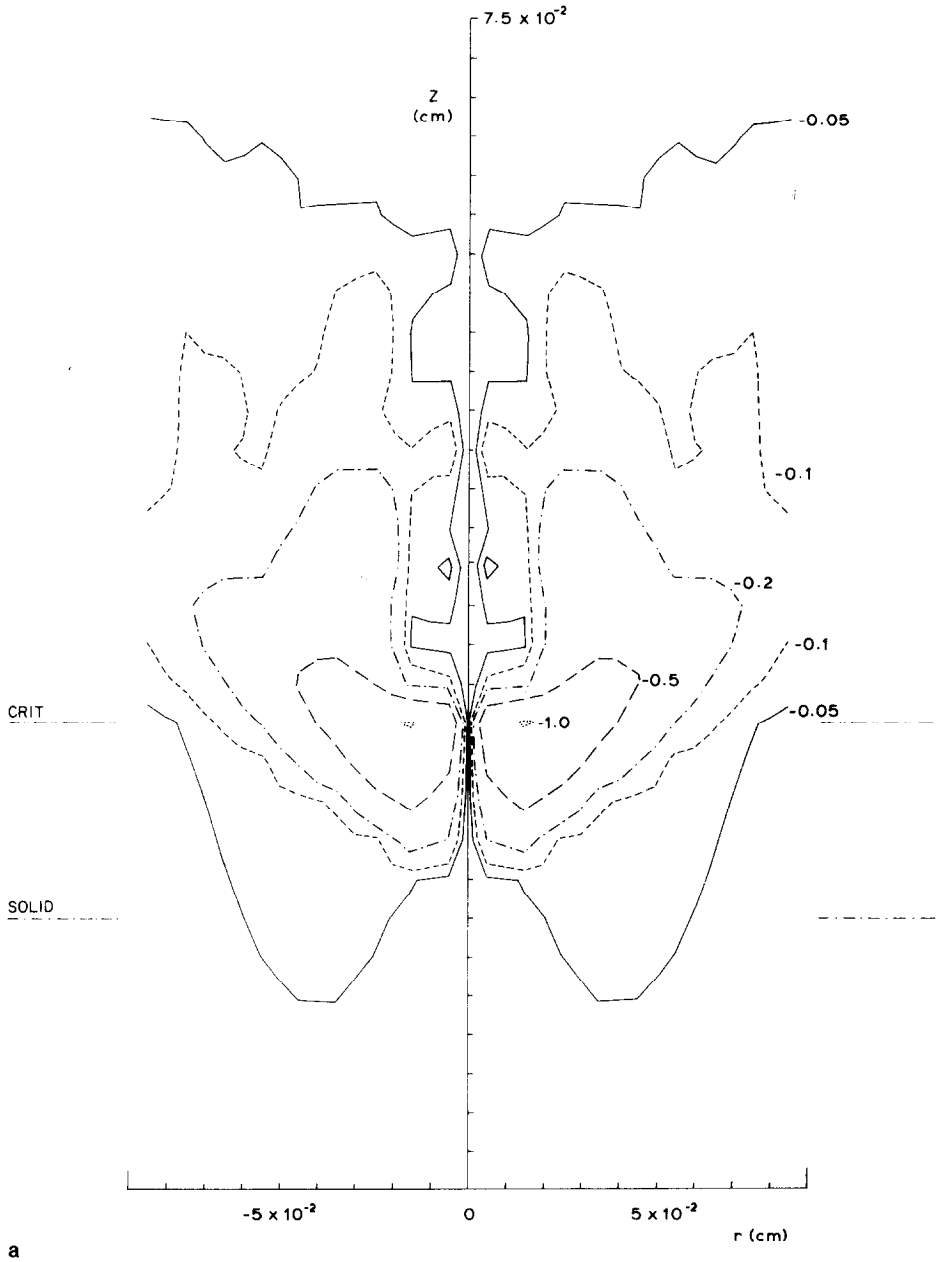

FIG. 3. The spatial distribution of magnetic field calculated with the positivity maintaining version of MAGT (*P*) under conditions described in the text, Section 11. Both contour map (a) and three dimensional plot (b) are shown. Units are megagauss.

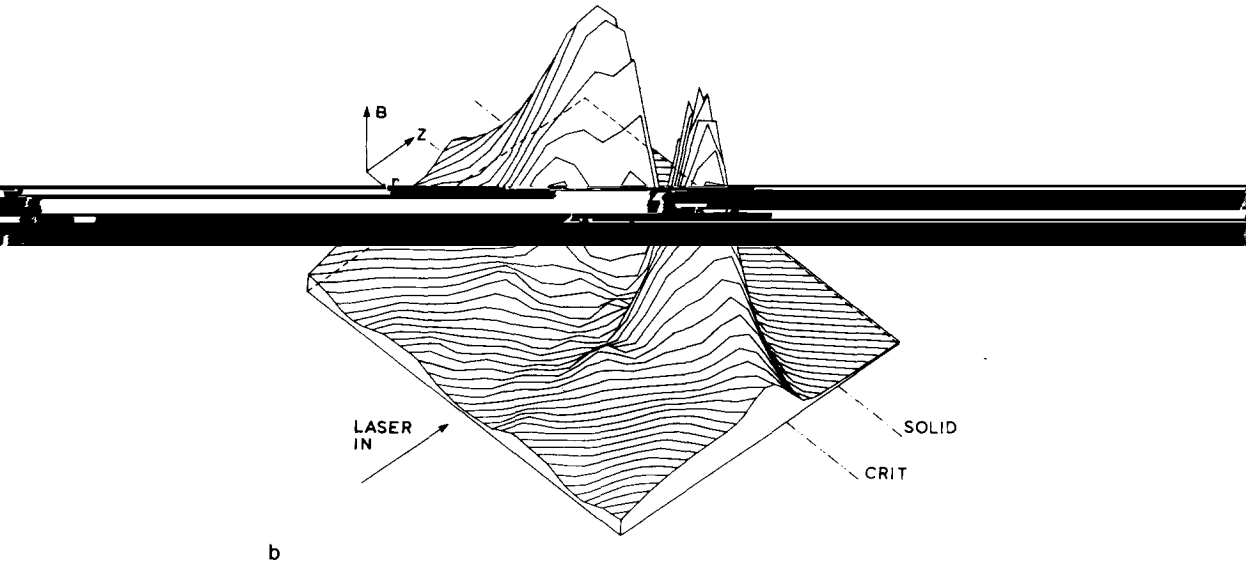

FIG. 3—*Continued.*

The laser beam consisted of a pulsed Gaussian in space and time with a radial $1/e$ width of 10 μm, temporal $1/e$ width equal to the time-to-peak of 100 psec and an intensity on axis of 10^{16} W/cm^2. The laser wavelength was 1.06 μm corresponding to a *Nd*: glass system. The accuracy factor, a, was set to 10^{-3}, the flux limiting factor, f, as defined in Ref. [28] to 0.63 and the reflectivity at the critical surface to 0.

For convenience we will present results at a single time only, 100 psec after the start of irradiation, i.e., at the peak of the laser pulse. We shall show only the behaviour of the most sensitive parameter, namely, the magnetic field. To fully illustrate the spatial variation we shall show both a contour map and a projection of the complete surface. In each case the surface is mapped on both sides of the cylindrical axis and allows the surface to be seen from both back and front in the projection, the axis of symmetry on the projections being shown by the arrow. The initial positions of the solid boundary and the critical density surface are indicated.

In Figs. 3 and 4 we compare the non-negativity preserving, P (Eq. (41)) and strongly conservative, C (Eq. (41a)) versions of the code for the case when the thermo-electric coefficients, β_0, are set to zero. As can be seen the two codes give very similar smooth and well-behaved results. The peak field for the form P is -1.02 MG contrasting with the value -1.22 MG for C, both occurring at the same point in space. The greatest difference occurs at the boundaries, where the fields are relatively small, but differ by up to a factor of 2; for example, in cell (1, 1) code P gives a value -8.41 kG compared to -15.4 kG for C. In contrast variations in the electron temperature, flow velocity and other parameters do not anywhere exceed 5%. Code C is slightly slower than code P. Thus P required 506 time-steps compared to 546 with C to reach 100 psec. The comparative CPU times using a CDC 7600 for

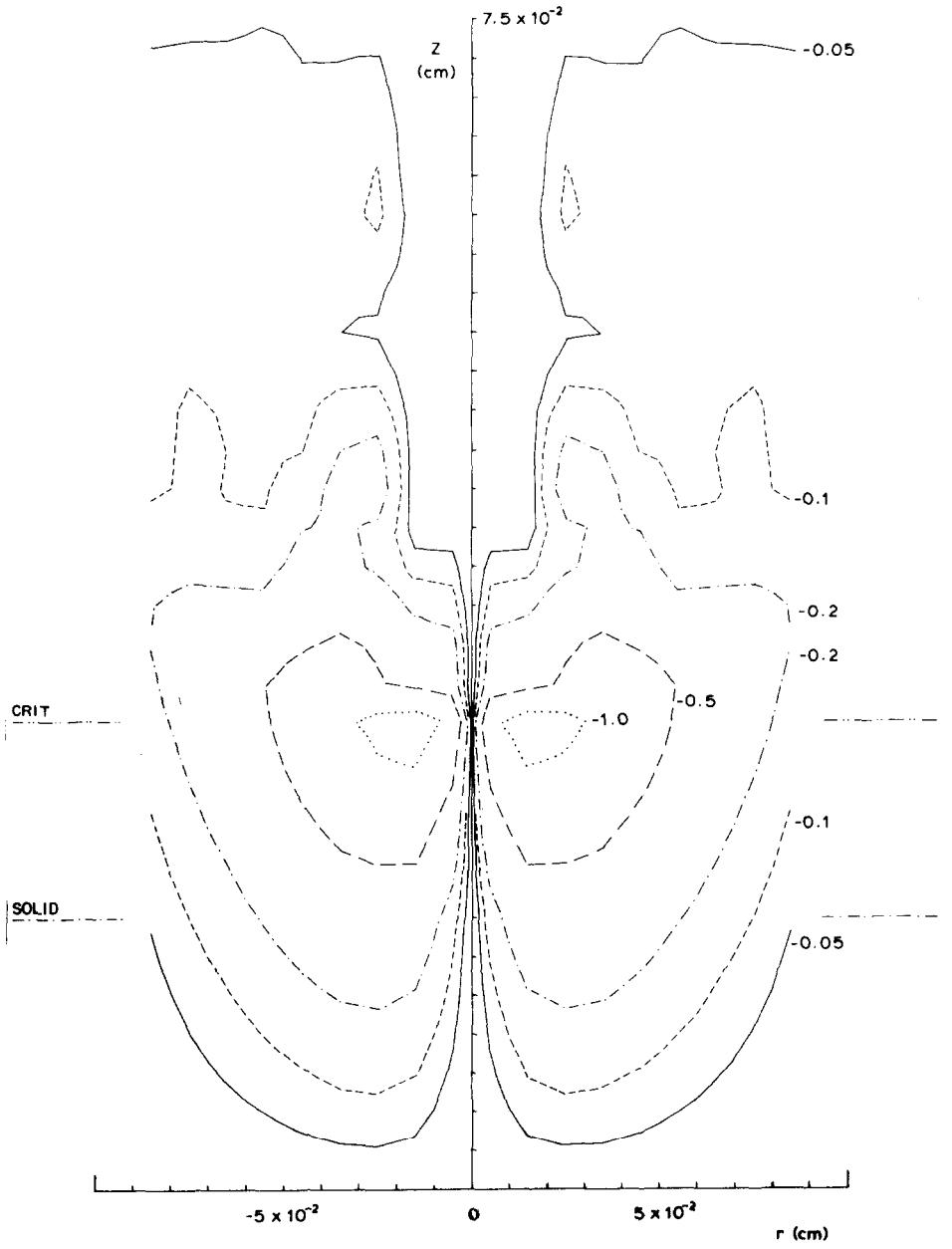

FIG. 4. Contour map of the magnetic field under conditions identical to those of Fig. 3 calculated with the conservative version of MAGT (*C*).

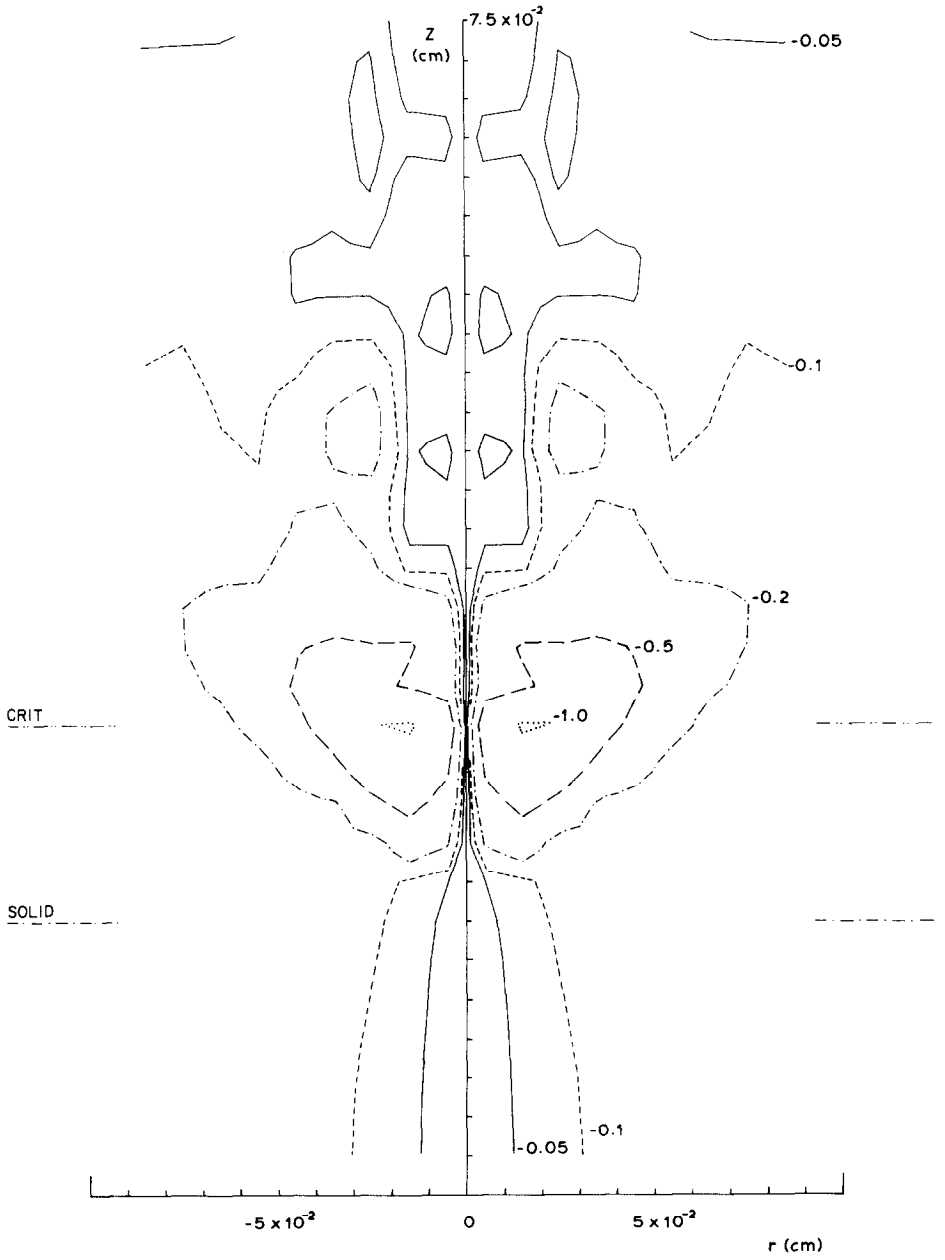

FIG. 5. Contour map of the magnetic field under conditions equivalent to those of Fig. 3, but calculated with a closed boundary for magnetic diffusion.

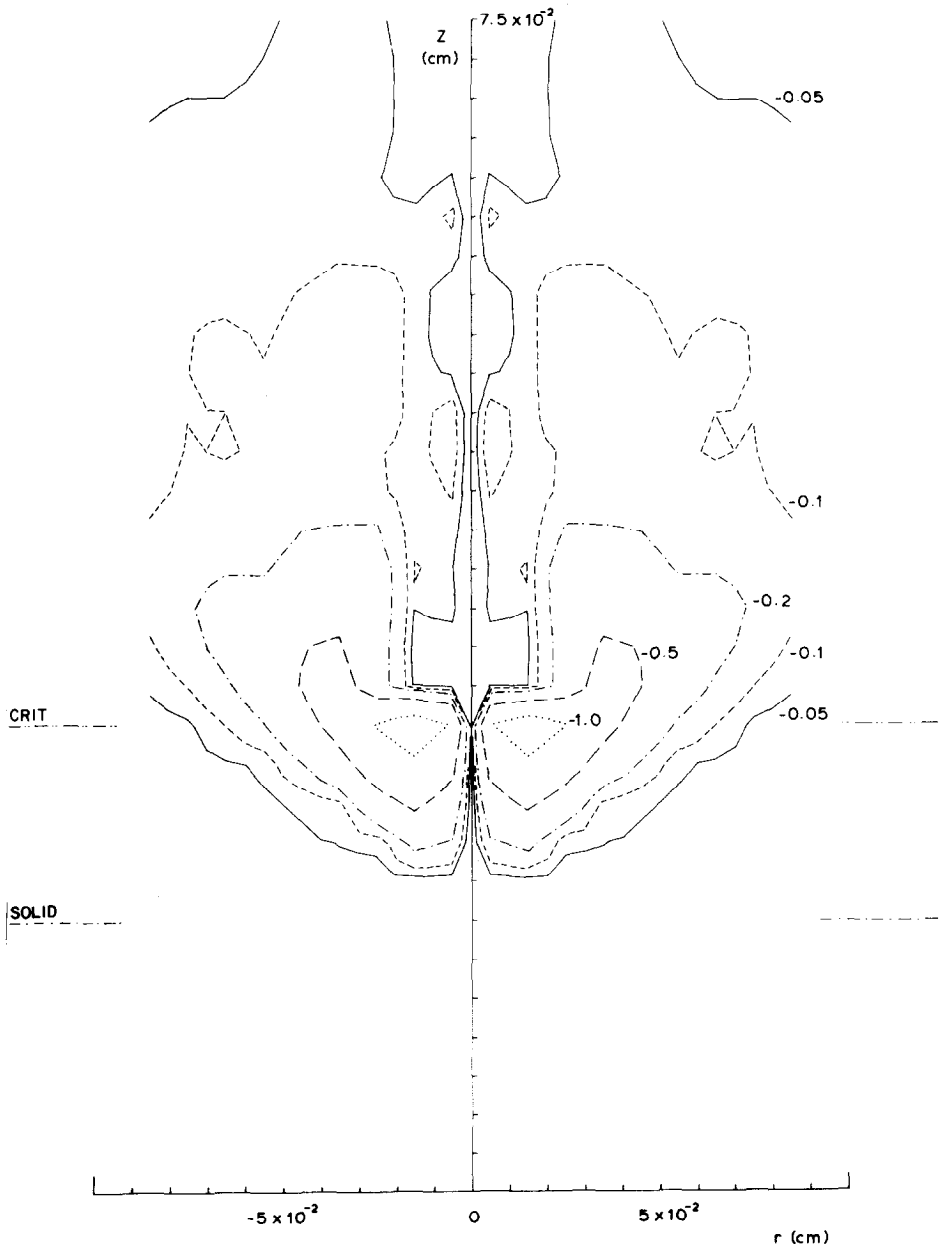

FIG. 6. Contour map of the magnetic field under conditions equivalent to those of Fig. 3, but calculated with an open boundary for magnetic diffusion.

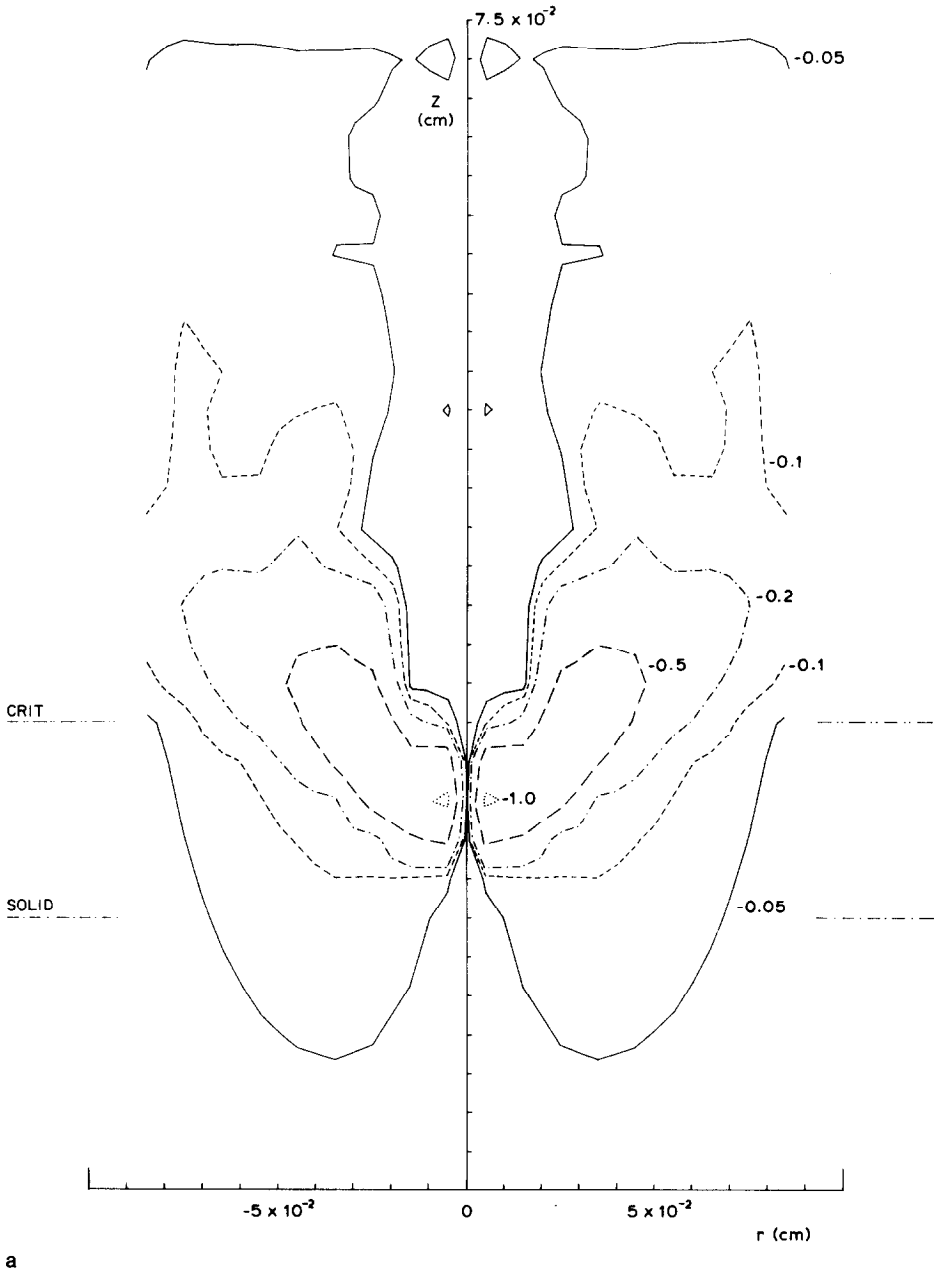

FIG. 7. The spatial distribution of magnetic field calculated with the full set of thermo-electric coefficients included under the same conditions as those of Fig. 3. Both the contour map (a) and three dimensional plot (b) are shown.

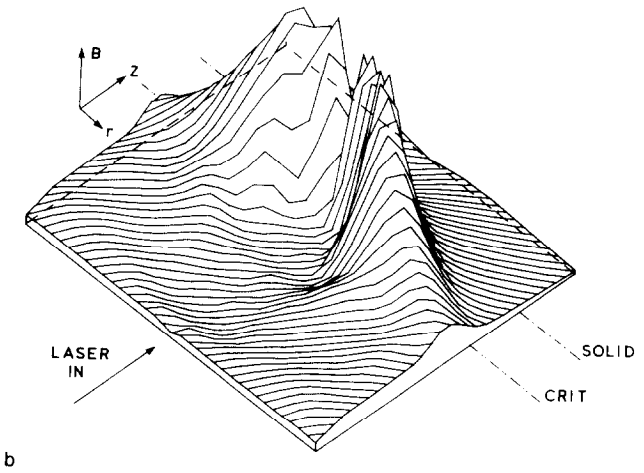

FIG. 7—*Continued.*

1000 time-steps were 562 (*P*) and 596 (*C*). Surprisingly the energy conservation error after approximately 500 time-steps was less for the positivity conserving form (15%) than for the strongly conservative one (17%), reflecting the conservation error associated with the iteration error in the matrix solving routines. For these reasons the non-negativity preserving form (*P*) is generally preferred, and was used in the subsequent tests reported here.

In Figs. 5 and 6 we compare the effect of differing boundary conditions on the diffusion of the magnetic field. Figure 5 shows the case of closed (reflective) boundary conditions, and Fig. 6 that of open with the boundary value in (124) set to zero, both calculations being performed with code *P* under conditions identical to those for Fig. 3, with which they should be compared. For comparison the closed form took 507 time-steps and had an energy conservation error of 15% after 100 psec, whereas the open calculation took 475 steps and had a similar error of 15% at the same time. Comparing Figs. 3, 5 and 6 it can be seen that over the major region of field generation, the boundaries have only a small influence, the peak fields being respectively -1.02, -1.03 and -1.30 MG, and occurring at the same point in space. At the boundaries the largest difference occurs in the solid at the edge of the mesh (1, 9), where the values are -15.0, -101.0, -1.19 kG, respectively. In contrast at the downstream corner (30, 9) the values show less variation, namely, -20.1, -32.5 and -20.5 kG, respectively. In general the precise form of the diffusion boundary is not significant, except for the region noted, where strong diffusion at the cold boundary is expected. The form described in Section 9 is intermediate between the two limiting cases and, in the author's opinion, gives the most satisfactory compromise.

The inclusion of the complete form of the tensor $\boldsymbol{\beta}$ considerably increases the running time of the code, primarily through a decrease in the time-step required to satisfy (90). The code, *P*, took 1601 time-steps, with an overall energy conservation

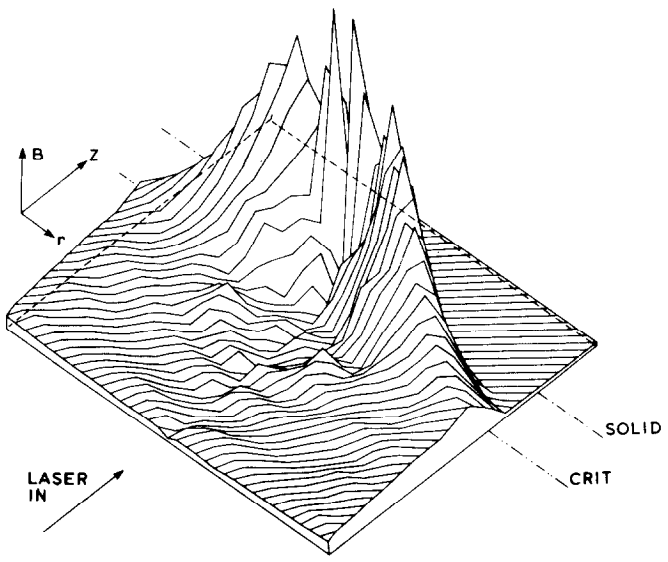

FIG. 8. Three dimensional plot of the magnetic field calculated under conditions similar to those of Fig. 7, but using an explicit form of the cross product term $\beta_{\wedge}$.

error of 24% to reach 100 psec. The comparative CPU time for the first 1000 steps was only 354 sec, reflecting the more rapid ICCG iteration with a shorter time-step. The magnetic fields generated at 100 psec are shown in Fig. 7. Comparison with Fig. 3 shows that although the general pattern of the field is not greately changed by the additional terms, the peak fields being -1.08 and -1.02 MG, respectively, significant differences in detail do occur, with the peak field occurring in cell (10, 1) in the full calculation compared with (13, 2) in the simpler case; the overall effect being to shift the fields into the solid. For comparison we show in Fig. 8 the result of a calculation for which $\beta_{\wedge}$ is treated by explicit centred difference, rather than (55). The marked irregularity thus introduced [illegible] although the overall pattern remains very similar.

In Fig. 9 we illustrate the modification to the solution introduced by Bohm diffusion instead of classical under the same conditions as those of Fig. 3. The marked increased in magnetic diffusion is clearly noticeable, but is accomplished without any adverse effects to the behaviour of the finite difference scheme.

The overall conservation errors recorded in these runs ($\sim$20%) are larger than those one would normally accept in a modelling calculation. The dominant source of error in this calculation is due to the errors accumulated in the iteration procedures, and is approximately proportional to a $\sqrt{N}$, where N is the number of time-steps. Since a could probably have been reduced to about 10^{-4} without significantly changing the step-length, Dt, an improvement of the overal conservation error to an acceptable 2% could readily have been accomplished, although with a corresponding increase in CPU time.

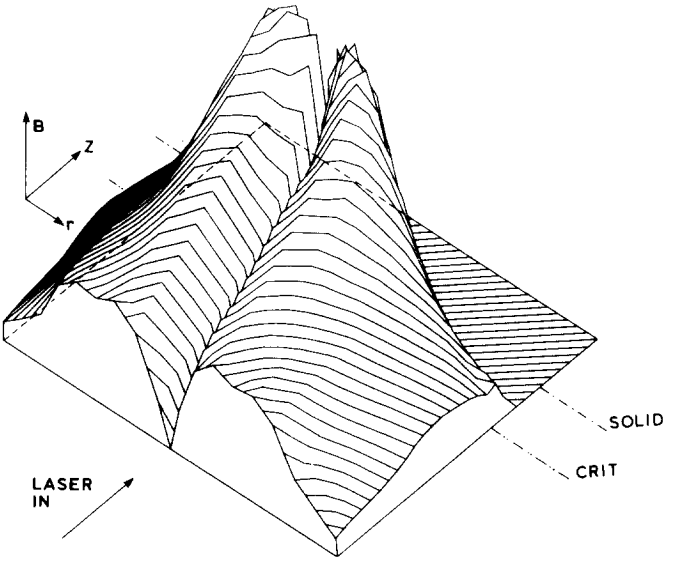

FIG. 9. Three dimensional plot of the magnetic field under conditions equivalent to those of Fig. 3, but with Bohm, instead of classical, magnetic diffusion.

12. CONCLUSIONS

The numerical modelling of self-generated magnetic fields, their diffusion and coupling with the overall hydrodynamic behaviour of a plasma has been considered. Algorithms suitable for the calculation of each aspect of the problem are described, and their properties analysed. It is shown that considerable care must be taken if the solution generated is to be well-behaved, stable and reasonably smooth. The incorporation of these algorithms into a complete working code has been described, and some typical solutions presented to indicate the general good behaviour of this code. In this form no additional smoothing has been found to be necessary during extensive experience with this code.

APPENDIX 1: VALUES OF PARAMETERS ON AXIS

On the axis of symmetry it follows from Ampère's law that the magnetic field must be zero:

$$B = 0: r = 0. \tag{A1.1}$$

Hence we may show from the known behaviour of the transport coefficients, and the governing equations that

v and B are odd in r,
d, u, E and H are even in r.

Thus if X is a general even variable,

$$\frac{\partial X}{\partial r} = 0 : r = 0. \tag{A1.2}$$

Expanding B in an odd power series in r we obtain

$$\frac{1}{r}\frac{\partial}{\partial r}(Br)\Big|_{r=0} \simeq 4B_{1/2}/\delta R \qquad \text{first term only,} \tag{A1.3a}$$

or

$$\simeq (27B_{1/2} - B_{3/2})/6\delta R \qquad \text{first two terms,} \tag{A1.3b}$$

where $B_{1/2}$ is the value of B at the centre of the cell $j = 0$. As described in the text the first term (a) is generally used.

Expanding X in even powers:

$$X|_{r=0} \simeq X_{1/2} \tag{A1.4a}$$

or

$$X|_{r=0} \simeq (9X_{1/2} - X_{3/2})/8. \tag{A1.4b}$$

Of these the second is more accurate, but requires a check to ensure positivity. The simpler form (A1.4a) has been used throughout for the flow variables. However, a modified form,

$$X|_{r=0} = \text{Max}\{(9X_{1/2} - X_{3/2})/8,\ 0.8X_{1/2}\}, \tag{A1.4c}$$

has been used to calculate the values of the even transport parameters on the axis.

In a similar fashion we note that the transport coefficients, $\alpha_\perp$, are even and $\alpha_\wedge$ are odd. Thus Eqs. (A1.4) may also be used for $\alpha_\perp$. For the cross product terms we note

$$\alpha_\wedge = \frac{\partial}{\partial r}\left(\frac{\alpha_\wedge}{r}\right) = \frac{\partial}{\partial r}(r\alpha_\wedge) = 0 : r = 0. \tag{A1.5}$$

In using these terms in the finite difference expressions, Eqs. (A1.1), (A1.2) and (A1.5) are exact and must be rigorously maintained. On the other hand, expressions (A1.3) to (A1.4) are approximate and may be used as required.

It is also implicit in (A1.5) that if Eq. (37) is obeyed,

$$\left(\frac{\alpha_\wedge}{r}\right)_{-1/2} = \left(\frac{\alpha_\wedge}{r}\right)_{1/2} = \left(\frac{\alpha_\wedge}{r}\right)_0$$

and

$$(\alpha_\wedge r)_{-1/2} = (\alpha_\wedge r)_{1/2} = (\alpha_\wedge r)_0 \tag{A1.6}$$

must be used to evaluate $\Delta(\alpha_\wedge/r)_0$ or $\Delta(\alpha_\wedge r)_0$ in Eqs. (93) and (107).

Appendix 2: The General Diffusion Equation as a Stiff Equation

The general diffusion equation in the presence of a magnetic field has the form

$$\frac{\partial \psi}{\partial t} = \nabla(\boldsymbol{\chi} \cdot \nabla\psi), \tag{A2.1}$$

where

$$\boldsymbol{\chi} \cdot \nabla\psi = \chi_{||}\nabla_{||}\psi + \chi_\perp \nabla_\perp \psi + \chi_\wedge \mathbf{h}_\wedge \nabla\psi. \tag{A2.2}$$

Since the field B has a constant direction, the following behaviour occurs at an extremum of ψ where $\nabla\psi = 0$.

$$\nabla \cdot (\chi_\wedge \mathbf{h}_\wedge \nabla\psi) = \nabla\psi \cdot \operatorname{curl}(\chi_\wedge \mathbf{h}) = 0 \tag{A2.3}$$

$$\therefore \frac{\partial \psi}{\partial t} = \nabla_{||}\{\chi_{||}\nabla_{||}\psi\} + \nabla_\perp\{\chi_\perp \nabla_\perp \psi\} = \chi_{||}\nabla_{||}^2\psi + \chi_\perp \nabla_\perp^2 \psi. \tag{A2.4}$$

At a maximum $\nabla_{||}^2\psi$ and $\nabla_\perp^2\psi$ are both negative

$$\begin{aligned} \therefore \frac{\partial \psi}{\partial t} &< 0 \qquad \text{at a maximum} \\ &> 0 \qquad \text{at a minimum} \end{aligned} \tag{A2.5}$$

Thus in general extrema decay in free diffusion [22, 29]. As a corollary no new extrema are spontaneously created.

Furthermore the extremum cannot maintain itself against decay by movement since if it moves with velocity $\mathbf{v}$

$$\frac{D\psi}{Dt} = \frac{\partial \psi}{\partial t} + \mathbf{v} \cdot \operatorname{grad} \psi = \frac{\partial \psi}{\partial t}. \tag{A2.6}$$

The finite difference representation of diffusion by means of a matrix equation in terms of the diffusion matrix, M, should therefore have the property that it creates no new maxima or minima in the field. A necessary condition is therefore one of positivity, namely, that the diffusion matrix be monotone. A form of matrix possessing this property is the M matrix form, where

$$M_{i,i} > 0, \qquad M_{i,j} \leqslant 0, \qquad i \neq j. \tag{A2.7}$$

In order to maintain the extremal property we make use of the result that if

$$A, B, C, D, E \geqslant 0 \qquad \text{and} \qquad C = A + B + D + E + F$$

then the solution X, of the equation

$$-AX_1 - BX_2 + CX - DX_3 - EX_4 = FX_0, \tag{A2.8}$$

satisfies

$$\text{Min}(X_0, X_1, X_2, X_3, X_4) < X < \text{Max}(X_0, X_1, X_2, X_3, X_4). \tag{A2.9}$$

Thus the extremal condition is satisfied if the diffusion matrix is an M matrix, whose elements obey

$$M_{I,J;I,J} = -M_{I,J;I,J-1} - M_{I,J;I,J+1} - M_{I,J;I-1,J} - M_{I,J;I+1,J} + F_{I,J;I,J}, \tag{A2.10}$$

where the finite difference form of the diffusion equation is

$$\sum_{I',J'} M_{I,J;I',J'} X^{n+1}_{I',J'} = F_{I,J;I,J} X^n_{I,J}. \tag{A2.11}$$

Inspection of Eqs. (93) and (107) shows that (A2.10) is satisfied by the forms proposed. However, for large values of the cross product rates, the M matrix form is not retained.

Consider the equation

$$\frac{\partial y}{\partial t} = \gamma \frac{\partial y}{\partial x} \tag{A2.12}$$

in the region (x_1, x_2) and suppose that y has fixed values y_1 and y_2 at x_1 and x_2, respectively. If y is a single valued function of x in the range x_1 to x_2, then at some intermediate point x, as $t \to \infty$,

$$y \to \begin{cases} y_2, & \gamma > 0, \\ y_1, & \gamma < 0, \end{cases} \qquad x_1 < x < x_2. \tag{A2.13}$$

Consider now the one dimensional cross product diffusion term

$$\frac{\partial \psi}{\partial t} = \frac{\partial \chi_\wedge}{\partial y} \frac{\partial \psi}{\partial x} \tag{A2.14}$$

having the form of (A2.12), which we write in finite difference form as

$$D\psi = \frac{Dt}{\delta y \, \Delta x} \delta \chi_\wedge \, \Delta \psi. \tag{A2.15}$$

If $\chi_\wedge$ is independent of x, then

$$\psi_i^{n+1} = \psi_i^n + \Gamma(\psi_{i+1} - \psi_{i-1}), \tag{A2.16}$$

where

$$\Gamma = \frac{Dt \cdot \delta\chi_{\wedge}}{2\delta y\, \Delta x}.$$

In a stiff form, where $|\Gamma| \gg 1$, ψ_i^{n+1} tends to some value, which may be positive or negative depending on the sign of Γ and the magnitudes of ψ_{i+1} and ψ_{i-1}. This is clearly unsatisfactory. However, Eq. (A2.13) suggests that in this case

$$\begin{aligned} &\Gamma \gg 1, \qquad \psi_i \to \psi_{i+1}, \\ &\Gamma \ll -1, \qquad \psi_i \to \psi_{i-1}. \end{aligned} \tag{A2.17}$$

This behaviour is ensured by replacing the centred space difference in (A2.16) by an appropriate forward or backward difference,

$$\begin{aligned} &\Gamma > 0: \qquad \psi_i^{n+1} = \psi_i^n + 2\Gamma(\psi_{i+1} - \psi_i) = \frac{\psi_i^n + 2\Gamma\psi_{i+1}^{n+1}}{1 + 2\Gamma}, \\ &\Gamma < 0: \qquad \psi_i^{n+1} = \psi_i^n + 2\Gamma(\psi_i - \psi_{i-1}) = \frac{\psi_i^n - 2\Gamma\psi_{i-1}^{n+1}}{1 - 2\Gamma}, \end{aligned} \tag{A2.18}$$

in a fully implicit form. Furthermore it can be seen that if used as in Eq. (A2.18) the diffusion matrix including the forward or backward difference has an M matrix form, and also satisfies Eq. (A2.10). We may further remark that this form is clearly closely compatible with the differencing form (35) for the derivatives. This simple device thus guarantees physical behaviour[1] for the solution of the diffusion equation. It is not, however, conservative and will thus lead to conservation errors which will modify the time step, if such a check is included.

The cross product diffusion terms can be shown to represent a reversible evolution of the system [22] in contrast to the direct terms, which are irreversible. The cross product terms alone thus give rise to a purely oscillatory behaviour. This behaviour is only maintained if the differencing of these terms is anti-symmetric [22] and a centred time-difference is used. The cross product terms in (107) are correctly symmmetrised, although not in (108), and if used alone with a centred time difference will yield a purely oscillatory solution, but with phase errors, whose size depends on the time-step used. The use of a fully implicit time-step, or upstream spatial differencing, damps these oscillatory modes. In practice one is only interested in oscillations whose period is comparable with the characteristic times in the problem, and one is content to average over more rapid variations. This desirable behaviour is achieved by the damping of rapid oscillations by the non-centred forms. The damping

[1] We note that in the case of magnetic field diffusion, if there is a change in sign between cells, e.g., $\Gamma \gg 1$, $B_{i+1}/B_i < 0$, then since $\eta_{\wedge} \to 0$ as $B \to 0$, $B_i \to 0$ (not B_{i+1}); i.e., the Hall effect does not induce a change in direction of the field.

of long period oscillations may be avoided by the use of the correctly symmetrised form (107) with a weighted time-difference to yield centred-time differencing for slowly varying events [22].

ACKNOWLEDGMENTS

I would like to thank A. J. Bennett for many helpful discussions concerning the code MAGT. Valuable comments from Dr. J. S. Christiansen are gratefully acknowledged. This work has been supported by a grant from the SRC Rutherford Laboratory.

REFERENCES

1. J. A. STAMPER, K. PAPADOPOLOUS, R. N. SUDAN, S. O. DEAN, E. A. MCLEAN, AND J. A. DAWSON, *Phys. Rev. Lett.* **26** (1971), 1012.
2. D. A. TIDMAN AND J. A. STAMPER, *Appl. Phys. Lett.* **22** (1973), 498.
3. G. J. PERT, *J. Plasma Phys.* **18** (1977), 227.
5. J. A. STAMPER, *Phys. Fluids* **19** (1976), 758.
6. B. BEZZERIDES, D. F. DUBOIS, AND D. W. FORSLUND, *Phys. Rev. A* **16** (1977), 1678.
7. P. LAX AND B. WENDROFF, *Comm. Pure Appl. Math.* **13** (1960), 217.
8. R. A. GENTRY, R. E. MARTIN, AND B. J. DALY, *J. Comput. Phys.* **1** (1966), 87.
9. J. P. BORIS AND D. L. BOOK, *J. Comput. Phys.* **11** (1973), 38.
10. D. L. BOOK, J. P. BORIS, AND K. HAIN, *J. Comput. Phys.* **18** (1975), 248.
11. D. G. COLOMBANT, K. G. WHITNEY, D. A. TIDMAN, N. K. WINSOR, AND J. DAVIS, *Phys. Fluids* **18** (1975), 1687.
12. R. S. CRAXTON, Ph.D. thesis, University of London.
13. J. B. CHASE, J. M. LEBLANC, AND J. R. WILSON, *Phys. Fluids* **16** (1973), 1142.
14. J. P. CHRISTIANSEN AND N. K. WINSOR, *J. Comput. Phys.* **35** (1980), 291.
15. K. V. ROBERTS AND D. E. POTTER, *in* "Methods in Computational Physics" (B. Alder, S. Fernback, and M. Rotenberg, Eds.), Vol. 9, p. 339, Academic Press, New York, 1970.
16. I. LINDEMUTH AND J. KILLEEN, *J. Comput. Phys.* **13** (1973), 181.
17. I. LINDEMUTH, *J. Comput. Phys.* **18** (1975), 119.
18. D. S. KERSHAW, *J. Comput. Phys.* **26** (1978), 43.
19. S. I. BRAGINSKII, *in* "Review of Plasma Physics" (M. A. Leontovich, Ed.), Vol. 1, p. 265, Consultant Bureau, New York, 1965.
20. L. SPITZER, JR., "Physics of Fully Ionised Gases," Interscience, New York, 1956.
21. J. P. CHRISTIANSEN AND K. V. ROBERTS, *J. Comput. Phys.* **17** (1975), 332.
22. G. J. PERT, *J. Comput. Phys.* **42** (1981), 20.
23. R. D. RICHTMYER AND K. W. MORTON, "Difference Methods for Initial Value Problems," Interscience, New York, 1967.
24. D. W. PEACEMAN AND H. H. RACHFORD, JR., *J. Soc. Ind. Appl. Math.* **3** (1955), 28.
25. J. DOUGLAS, JR., AND J. E. GUNN, *Numer. Math.* **6** (1964), 428.
26. J. P. CHRISTIANSEN AND K. V. ROBERTS, *J. Comput. Phys.* **28** (1978), 279.
27. G. J. PERT, "Laser–Plasma Interactions" (R. A. Cairns and J. J. Sanderson, Eds.), p. 323, Scottish Univ. Summer School Press, Edinburgh, 1980.
28. R. C. MALONE, R. L. MCCORY, AND R. L. MORSE, *Phys. Rev. Lett.* **34** (1975), 721.
29. P. M. MORSE AND H. FESHBACK, "Methods of Theoretical Physics," McGraw–Hill, New York, 1953.